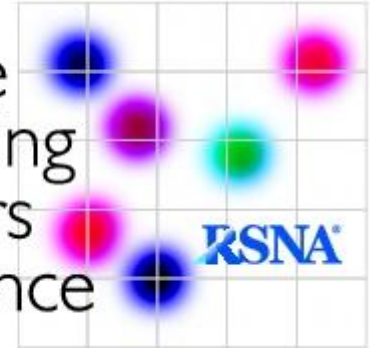


Quantitative
Imaging
Biomarkers
Alliance



QIBA Profile: Diffusion-Weighted Magnetic Resonance Imaging (DWI)

Stage: A. Initial Draft

Notation in this Template

| Template Element | Appears as | Instructions |
|------------------|-------------------------------------|------------------------------------------------------------------------------------------------------------------------------------------------------------------------------|
| Boilerplate text | Plain black text | Don't change. Should appear in all profiles. |
| Example text | Plain grey text | Provides an example of content and wording appropriate to that location. Rewrite it to your needs and change the text color back to Automatic (which will make it black). |
| Placeholder | <text in angle brackets> | Replace text and <> with your text. Use Find/Replace for ones that appear frequently. |
| Guidance | Comment with "GUIDANCE" at the top. | Delete it when you've followed it and don't need it anymore. |

Table of Contents

| | | | |
|----|--------------------------------------------------|--|----|
| 15 | | | |
| 16 | Change Log: | | 4 |
| 17 | Open Issues: | | 4 |
| 18 | Closed Issues: | | 5 |
| 19 | 1. Executive Summary | | 6 |
| 20 | 2. Clinical Context and Claims | | 7 |
| 21 | 3. Profile Activities | | 10 |
| 22 | 3.1. Pre-delivery | | 11 |
| 23 | 3.1.1 Discussion | | 11 |
| 24 | 3.2. Installation | | 11 |
| 25 | 3.2.1 Discussion | | 11 |
| 26 | 3.3. Periodic QA | | 11 |
| 27 | 3.3.1 Discussion | | 11 |
| 28 | 3.3.2 Specification | | 12 |
| 29 | 3.4. Subject Selection | | 12 |
| 30 | 3.4.1 Discussion | | 12 |
| 31 | 3.5. Subject Handling | | 12 |
| 32 | 3.5.1 Discussion | | 12 |
| 33 | 3.6. Image Data Acquisition | | 13 |
| 34 | 3.6.1 Discussion | | 13 |
| 35 | 3.6.2 Specification | | 13 |
| 36 | 3.7. Image Data Reconstruction | | 18 |
| 37 | 3.7.1 Discussion | | 18 |
| 38 | 3.7.2 Specification | | 18 |
| 39 | 3.8. Image QA | | 19 |
| 40 | 3.8.1 Discussion | | 19 |
| 41 | 3.8.2 Specification | | 20 |
| 42 | 3.9. Image Distribution | | 20 |
| 43 | 3.9.1 Discussion | | 20 |
| 44 | 3.9.2 Specification | | 20 |
| 45 | 3.10. Image Analysis | | 20 |
| 46 | 3.10.1 Discussion: ROI definition in DWI imaging | | 21 |
| 47 | 3.10.1.1 Brain | | 21 |
| 48 | 3.10.1.2 LIVER | | 21 |
| 49 | 3.10.1.3 PROSTATE | | 22 |

| | | |
|----|----------------------------------------------------------------------------|----|
| 50 | 3.10.2 Specification | 22 |
| 51 | 3.11. Image Interpretation | 22 |
| 52 | 3.11.1 Discussion | 22 |
| 53 | 4. Assessment Procedures | 24 |
| 54 | 4.1. Assessment Procedure: MRI Equipment Specifications and Performance | 24 |
| 55 | 4.2. Assessment Procedure: Technologist | 24 |
| 56 | 4.3. Assessment Procedure: Radiologists | 25 |
| 57 | 4.4. Assessment Procedure: Image Analyst / Physicist / Scientist | 25 |
| 58 | 4.5. Assessment Procedure: Image Analysis Software | 25 |
| 59 | References | 27 |
| 60 | Appendices | 33 |
| 61 | Appendix A: Acknowledgements and Attributions | 33 |
| 62 | Appendix B: Background Information | 33 |
| 63 | Appendix C: Conventions and Definitions | 34 |
| 64 | Appendix D: Platform-Specific Acquisition Parameters for DWI Phantom Scans | 35 |
| 65 | Appendix E: Technical Assessment Procedures | 38 |
| 66 | E.1. Assessment Procedure: ADC QUALITIES AT/NEAR Isocenter | 39 |
| 67 | E.1.1 Discussion | 39 |
| 68 | E.1.2 Specification | 40 |
| 69 | E.2. Assessment Procedure: DWI Signal to Noise | 41 |
| 70 | E.2.1 Discussion | 41 |
| 71 | E.2.2 Specification | 43 |
| 72 | E.3. Assessment Procedure: ADC <i>b</i> -value dependence | 44 |
| 73 | E.3.1 Discussion | 44 |
| 74 | E.3.2 Specification | 44 |
| 75 | E.4. Assessment Procedure: ADC spatial dependence | 44 |
| 76 | E.4.1 Discussion | 44 |
| 77 | E.4.2 Specification | 45 |
| 78 | | |
| 79 | | |
| 80 | | |
| 81 | | |
| 82 | | |

83

84 **Change Log:**

85 This table is a best-effort of the authors to summarize significant changes to the Profile.

86

| Date | Sections Affected | Summary of Change |
|------------|--------------------------------|---------------------------------------------------------------------------------------------------------------------------------------------------------------------------------------------------------------------------|
| 2015.10.10 | All | Major cleanup based on comments resolved in the Process Cmte. Also had to remove a few hundred extraneous paragraph styles. |
| 2015.10.21 | All | Approved by Process Cmte |
| 2015.11.04 | 2 (Claims) 3 (Requirements) | Incorporating the more refined form of the claim language and referenced a separate claim template. Added Voxel Noise requirement to show example of the linkage between the requirement and the assessment procedure. |
| 2015.12.16 | | Minor changes to remove reference to "qualitative" measurements, fix reference to guidance and clean some formatting. |
| 2016.01.06 | 1, 3.8.1 | Rewording to avoid the term "accuracy". |
| 2016.11.21 | 2 | Removed polygonal brain ROI area reference (not literature-supported) |
| 2017.01.18 | All | Endnote library of references, prostate added, reconciled ToC with actual content, fixed formatting, cleaned up most comments and highlights, ready for PDF review |

87

88 **Open Issues:**

89 The following issues are provided here to capture associated discussion, to focus the attention of
 90 reviewers on topics needing feedback, and to track them so they are ultimately resolved. In particular,
 91 comments on these issues are highly encouraged during the Public Comment stage.

| |
|------------------------------------------------------------------------------------------------------------------------------------------------------------------------------------------------------------------------------------------------------------|
| <p>Q. Who to include in Appendix B A. RSNA staff has provided current roster, this is an issue that can be addressed in Google Docs while PDF is reviewing, with a final review at the BC level prior to handoff to MR CC.</p> |
| <p>Q. Comments in Prostate Section A. As the most recently edited organ section, we ask PDF readers to examine the claims and justifications prior to moving up to the MR CC level.</p> |
| <p>Q. Include images of relevant artifacts for Image QA section 3.8 A. While PDF is reviewing, the TF members will look for appropriate examples of DWI artifacts in brain, liver and prostate to include in Appendix</p> |

92

93

94

95 **Closed Issues:**

96 The following issues have been considered closed by the biomarker committee. They are provided here
 97 to forestall discussion of issues that have already been raised and resolved, and to provide a record of
 98 the rationale behind the resolution.

| |
|--------------------------------------------------------------------------------------------------------------------------------------------------------------------------------------------------------------------------------------------------------------------------------------------------------------------------------------------------------------------------------------------------------------------------------------------------------------------------------------------------------------------------------------------------------------------------------------------------------------------------------------|
| <p>Q. Which organs have sufficient reproducibility literature for inclusion in the longitudinal claim statement?</p> <p>A. Organs for inclusion are brain, liver, and prostate. The following organs were considered, but have been excluded for the time being due to lack of sufficient literature (test-retest data from a total of ~35 subjects, either from a single publication or in total from multiple manuscripts) support:</p> <ul style="list-style-type: none"> Bone Breast Kidney Lymphoma Pancreas Head and neck Lung Whole Body |
| <p>Q. How much of the Subject Handling subsection (3.1) is applicable to DWI?</p> <p>A. Text has been adjusted according to standard clinical practice, subject to public review</p> |
| <p>Q. Should organ-specific protocols be changed to the profile template’s table format, or left as-is?</p> <p>A. Protocols were adapted for the three organs discussed in the first DWI profile.</p> |
| <p>Q. Can references be better formatted?</p> <p>A. Now using EndNote Library in Word, not sure how this will translate to Google Docs.</p> |
| <p>Q. How to make conformance section conform?</p> <p>A. Old Conformance section moved mostly to Appendices, current structure reflects profile template from Process Committee</p> |
| <p>Q. What DICOM parameters should be specified in section 3.2.2?</p> <p>A. In public tags, vendors should provide: <i>b</i>-value; diffusion gradient direction (3-vector) or “isotropic”; sequence class (single spin-echo monopolar; single spin-echo bipolar; double spin-echo bipolar; stimulated echo); This was addressed, section is now 3.6</p> |

99
 100
 101
 102

103 **1. Executive Summary**

104 The goal of a QIBA Profile is to help achieve a useful level of performance for a given biomarker. The **Claim**
105 (Section 2) describes the biomarker performance. The **Activities** (Section 3) contribute to generating the
106 biomarker. Requirements are placed on the **Actors** that participate in those activities as necessary to
107 achieve the Claim. **Assessment Procedures** (Section 4) for evaluating specific requirements are defined as
108 needed to ensure acceptable performance.

109 Diffusion-Weighted Imaging (DWI) and the Apparent Diffusion Coefficient (ADC) are being used clinically
110 as qualitative indicators of disease presence, progression or response to treatment [1-29] . Use of ADC as
111 a robust quantitative biomarker with finite confidence intervals places additional requirements on
112 Acquisition Devices and Protocols, Technologists, Radiologists, Scientists, Reconstruction Software and
113 Image Analysis Tools [30-37]. All of these are considered **Actors** involved in **Activities** of Subject Handling,
114 Image Data Acquisition, Reconstruction, Quality Assurance (QA) and Analysis. The requirements
115 addressed in this Profile are focused on achieving ADC values within a known (ideally negligible) systematic
116 bias range and avoiding unnecessary technical measurement variability [34, 36, 37].

117 **DISCLAIMER:** Technical performance of the MRI system can be assessed using a phantom having known
118 diffusion properties, such as the QIBA DWI phantom. The clinical performance target is to achieve a 95%
119 confidence interval for measurement of ADC with a variable precision depending on the organ being
120 imaged and assuming adequate technical performance requirements are met. While in vivo DWI/ADC
121 measurements have been performed throughout the human body, this Profile focused on three organ
122 systems, namely brain, liver, and prostate as having high clinical utilization of ADC with a sufficient level
123 of statistical evidence to support the Profile Claims derived from the current (as of March 2017) peer-
124 reviewed literature. In due time, new DWI technologies with proven greater performance levels, as well
125 as more organ systems will be incorporated in future Profiles.

126 Three levels of compliance for the current DWI profile specifications are defined as:

127 **ACCEPTABLE:** Failing to meet this specification will result in data that is likely unacceptable for the
128 intended use of this profile.

129 **TARGET:** Meeting this specification is achievable with reasonable effort and adequate equipment and is
130 expected to provide better results than meeting the ACCEPTABLE specification.

131 **IDEAL:** Meeting this specification may require extra effort or non-standard hardware or software, but is
132 expected to provide better results than meeting the TARGET.

133 This document is intended to help a variety of users: clinicians using this biomarker to aid patient
134 management; imaging staff generating this biomarker; MRI system architects developing related
135 products; purchasers of such products; and investigators designing clinical trials utilizing quantitative
136 diffusion-based imaging endpoints.

137 Note that this document only states requirements to achieve the claim, not requirements that pertain to
138 clinical standard of care.” Conforming to this Profile is secondary to proper patient care.

139

140

141 2. Clinical Context and Claims

142 Clinical Context

143 The goal of this profile is to facilitate appropriate use of quantitative diffusion weighted imaging (DWI) to
144 gain insight into the microstructure and composition of lesions in humans using precise quantitative
145 measurements of the apparent diffusion coefficient (ADC) for robust tissue characterization and
146 longitudinal tumor monitoring. The premise for its use is that therapy-induced cellular necrosis should
147 pre-date macroscopic lesion size change, thereby motivating exploration of ADC as a response biomarker
148 [3, 5, 6, 13, 14, 16, 18, 19, 22, 26, 27, 38, 39]. Within days to weeks after initiation of effective cytotoxic
149 therapy, tumor necrosis occurs, with a loss of cell membrane integrity and an increase of the extracellular
150 space typically resulting in a relative increase in ADC. During the following weeks to months, the tumor
151 may show shrinkage with a resorption of the free extracellular fluid and fibrotic conversion leading to a
152 decrease of the ADC, although tumor recurrence can also result in reduced ADC [21, 40, 41].

153
154 The objective of this Profile is to provide prerequisite knowledge of the expected level of variance in ADC
155 measurement unrelated to treatment, in order to properly interpret observed change in ADC following
156 treatment [30, 34, 36].

157
158 This QIBA DWI Profile makes Claims about the confidence with which ADC values and changes in a lesion
159 can be measured under a set of defined image acquisition, processing, and analysis conditions. It also
160 provides specifications that may be adopted by users and equipment developers to meet targeted levels
161 of clinical performance in identified settings. The intended audience of this document includes
162 healthcare professionals and all other stakeholders invested in the use of quantitative diffusion
163 biomarkers for treatment response and monitoring, including but not limited to:

- 164 ● Radiologists, technologists, and physicists designing protocols for ADC measurement
- 165 ● Radiologists, technologists, physicists, and administrators at healthcare institutions considering
166 specifications for procuring new MR equipment
- 167 ● Technical staff of software and device manufacturers who create products for this purpose
- 168 ● Biopharmaceutical companies
- 169 ● Clinicians engaged in therapy response monitoring
- 170 ● Clinical trialists
- 171 ● Radiologists and other health care providers making quantitative measurements on ADC maps
- 172 ● Oncologists, urologists, neurologists, other clinicians, regulators, professional societies, and others
173 making decisions based on quantitative diffusion image measurements
- 174 ● Radiologists, health care providers, administrators and government officials developing and
175 implementing policies for brain, liver, and prostate cancer treatment and monitoring

176
177 **Conformance to this Profile by all relevant staff and equipment supports the following claim(s):**

178

179 **Claim 1a: A measured change in the ADC of a brain lesion of 11% or larger indicates that**
180 **a true change has occurred with 95% confidence.**

181 **Claim 2a: A measured change in the ADC of a liver lesion of 26% or larger indicates that**
182 **a true change has occurred with 95% confidence.**

183 **Claim 3a: A measured change in the ADC of a prostate lesion of 47% or larger indicates**
 184 **that a true change has occurred with 95% confidence.**

185 -----

186 **Claim 1b: A 95% CI for the true change in ADC of a brain lesion is given below, where Y_1**
 187 **and Y_2 are the ADC measurements at the two time points:**

188
$$(Y_2 - Y_1) \pm 1.96 \times \sqrt{(Y_1 \times 0.040)^2 + (Y_2 \times 0.040)^2}.$$

189 **Claim 2b: A 95% CI for the true change in ADC of a liver lesion is given below, where Y_1**
 190 **and Y_2 are the ADC measurements at the two time points:**

191
$$(Y_2 - Y_1) \pm 1.96 \times \sqrt{(Y_1 \times 0.094)^2 + (Y_2 \times 0.094)^2}.$$

192 **Claim 3b: A 95% CI for the true change in ADC of a prostate lesion is given below, where**
 193 **Y_1 and Y_2 are the ADC measurements at the two time points:**

194
$$(Y_2 - Y_1) \pm 1.96 \times \sqrt{(Y_1 \times 0.17)^2 + (Y_2 \times 0.17)^2}.$$

195

196 **These claims hold when:**

- 197 ● The same imaging methods on the same scanner and the same analysis methods are used at two
 198 separate time points where the interval between measurements is intended to represent the
 199 evolution of the tissue over the interval of interest (such as pre-therapy versus post initiation of
 200 therapy).
- 201 ● Conspicuity of lesion boundary is adequate to localize the lesion for definition on a region-of-
 202 interest [27] at both time points.

203

204 **Discussion**

205

- 206 ● These claims are based on estimates of the within-subject coefficient of variation (wCV) for ROIs
 207 drawn in the brain, liver and prostate. For estimating the critical % change, the % Repeatability
 208 Coefficient (%RC) is used: $2.77 \times wCV \times 100\%$, or %RC = 11% for brain, 26% for liver, 47% for
 209 prostate. Specifically, it is assumed that the wCV is 4% for brain, 9% for liver, and 17% for prostate.
 210 The claim assumes that the wCV is constant for tissue regions in the specified size, the signal-to-
 211 noise ratio (SNR) of the tissue region on the $b=0$ image is at least 50, and that the measured ADC
 212 is linear (slope=1) with respect to the true ADC value over the range $0.25 \times 10^{-3} \text{ mm}^2/\text{s}$ to 2.5×10^{-3}
 213 mm^2/s .
- 214 ● For the brain, estimates are from Bonekamp 2007, Pfefferbaum 2003 (mean ADC in an anatomical
 215 region or polygonal ROI), and Paldino 2009 [42-44]; for the liver, estimates are from Miquel 2012,
 216 Braithwaite 2009 (mean ADC in an ROI between 1-4 cm^2) [45-48]; for the prostate, estimates are
 217 from Litjens 2012 and Gibbs 2007 (Table 1 of the manuscript, mean ADC is from an ROI ranging
 218 from 120 to 320 mm^2 , with little impact on repeatability) [49-52].

219

220 In tumors, changes in ADC can reflect variations in cellularity, as inferred by local tissue water mobility,
221 e.g., a reduction or increase of the extracellular space, although the level of measured change must be
222 interpreted relative to the Repeatability Coefficient before considered as a true change [1, 30, 34, 37,
223 53-55]. Other biological processes may also lead to changes in ADC, e.g., stroke.

224 While the Profile Claims have been informed by a review of the literature and expert consensus, the Claims
225 have not yet been fully substantiated by studies that strictly conform to the specifications given here. The
226 expectation is that during field test, data on the actual field performance will be collected and any
227 appropriate changes made to the claim or the details of the Profile. At that point, this caveat may be
228 removed or re-stated.

229

230

231

232 **3. Profile Activities**

233 The Profile is documented in terms of “Actors” performing “Activities”. Equipment, software, staff or sites
 234 may claim conformance to this Profile as one or more of the “Actors” in the following table.

235 Conformant Actors shall support the listed Activities by conforming to all requirements in the referenced
 236 Section.

237 **Table 1: Actors and Required Activities**

| Actor | Activity | Section |
|------------------------------------------------------|---------------------------------|---------------|
| Acquisition Device / Physicist / Field Engineer | Pre-delivery & Installation | 3.1. & 3.2. |
| | Periodic QA | 3.3. |
| | Image Data Acquisition | 3.6. |
| MR Technologist / Physicist / Scientist | Subject Selection & Handling | 3.4. & 3.5. |
| | Image Data Acquisition | 3.6. |
| | Image Data Reconstruction | 3.7. |
| Radiologist Image Analyst / Physicist / Scientist | Image QA | 3.8. |
| | Image Distribution | 3.9. |
| | Image Analysis & Interpretation | 3.10. & 3.11. |
| Reconstruction Software | Image Data Reconstruction | 3.7. |
| Image Analysis Tool | Image Analysis | 3.10. |

238

239 The requirements in this Profile do not codify a Standard of Care; they only provide guidance intended to
 240 achieve the stated Claim. Failing to conform to a “shall” statement in this Profile is a protocol deviation.
 241 Although deviations invalidate the Profile Claim, such deviations may be reasonable and unavoidable and
 242 the radiologist or supervising physician is expected to do so when required by the best interest of the
 243 patient or research subject. Handling protocol deviations for specific trials/studies is at full discretion of
 244 the study sponsors and other responsible parties.

245 The sequencing of Activities specified in this DWI Profile is shown in Figure 1:

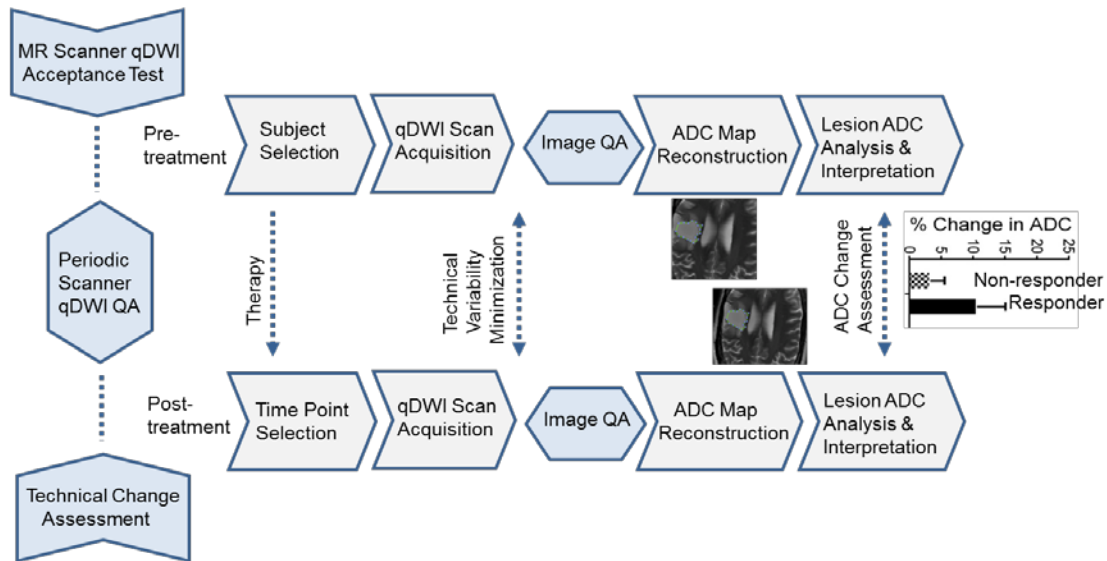


Figure 1: Diffusion-Weighted MRI for Treatment Response Assessment - Activity Sequence

246
247
248

3.1. Pre-delivery

This activity describes calibrations, phantom imaging, performance assessments or validations prior to delivery of equipment to a site (e.g. performed at the factory) that are necessary to reliably meet the Profile Claim.

3.1.1 DISCUSSION

Current clinical MR scanners with DWI capabilities are adequate. No additional specific pre-delivery activities are required for this Profile.

3.2. Installation

This activity describes calibrations, phantom imaging, performance assessments or validations that are part of commissioning acceptance testing and follow installation of equipment at the site that are necessary to reliably meet the Profile Claim.

3.2.1 DISCUSSION

Installation needs to be done by a trained field service engineer as per manufacturers' specifications and supervised by a local MR physicist. No additional specific installation activities are required by this Profile.

3.3. Periodic QA

This activity describes phantom imaging, performance assessments or validations performed periodically at the site, but not directly associated with a specific subject, that are necessary to reliably meet the Profile Claim.

3.3.1 DISCUSSION

Quality assurance procedures shall be consistent with those generally accepted for routine clinical imaging. The imaging device should have periodic performance assessment using methods and procedures defined by the MRI vendor, or other nationally/internationally recognized bodies such as

267
268
269
270

271 American Association of Physicists in Medicine (AAPM) [56], American College of Radiology (ACR), The
 272 Joint Commission or corresponding organizations in other countries. Preventive maintenance at
 273 appropriate regular intervals shall be conducted and documented by a qualified service engineer as
 274 recommended by the scanner manufacturer. Additional, DWI-specific QA procedures to ensure baseline
 275 scanner performance with minimal technical variability are described in Section 4 and Appendix D and E,
 276 and can be utilized as needed [21, 57].

277 3.3.2 SPECIFICATION

| Parameter | Actor | Requirement |
|------------------------------|----------------------------------------|---------------------------------------------------------------------------------------------------------------------------------------------------------------------------------|
| Accreditation of site/system | Physicist / Scientist | Shall be performed by a Qualified MRI Medical Physicist or MRI scientist as defined by appropriate accrediting bodies |
| System performance metrics | Field Engineer / Physicist / Scientist | System shall perform within vendor-established performance benchmark ranges for the given scanner model |
| Periodic DWI QC | Physicist / Scientist | Shall perform periodic system QC that includes assessment of ADC bias, random error, linearity, DWI SNR, DWI image artifacts, <i>b</i> -value dependence and spatial uniformity |

278

279 **3.4. Subject Selection**

280 This activity describes criteria and procedures related to the selection of appropriate imaging subjects that
 281 are necessary to reliably meet the Profile Claim.

282 3.4.1 DISCUSSION

283 All subjects considered safe for clinical MRI may be considered for a DWI study. Implants and devices
 284 categorized with status “MR Unsafe” are considered an absolute contraindication [58-61]. Implants and
 285 devices having status “MR Safe” or “MR Conditional” shall be evaluated per local MRI safety review
 286 procedures to assess relative risk status. Despite having an acceptable risk status, metal-containing
 287 implants and devices near the tissue/organ/lesion of interest may introduce artifact and may not be
 288 suitable for DWI. Contraindications unrelated to implants should be considered as well. These include
 289 but are not limited to: 1st trimester pregnancy, claustrophobia, age and subject’s ability to cooperate [62-
 290 65].

291 For specific study/trial, subject scan timing should be appropriately synchronized with the assayed subject
 292 condition (e.g., clinical state or therapeutic phase) per study design.

293 **3.5. Subject Handling**

294 This activity describes details of handling imaging subjects that are necessary to reliably meet the Profile
 295 Claim.

296 3.5.1 DISCUSSION

297 DWI patients should be prepared according to local standard of care (e.g. safety screening and removal of
 298 all metal objects and electronic devices) [58-60, 66]; otherwise no additional specific patient preparation
 299 procedures are required. Patients should wear appropriate attire (site-provided scrubs are preferred) and

300 be comfortably positioned to minimize patient motion and stress, which might affect the imaging results.
 301 At present, there is no consensus concerning all patient preparation issues.

302 To reduce motion artifact from bowel peristalsis during prostate imaging, the use of an antispasmodic
 303 agent may be beneficial in some patients. However, in many others it is not necessary, and the incremental
 304 cost and potential for adverse drug reactions should be taken into consideration. The presence of stool in
 305 the rectum may interfere with placement of an endorectal coil. If an ERC is not used, the presence of air
 306 and/or stool in the rectum may induce artifactual distortion that can compromise DWI quality. Thus, some
 307 type of minimal preparation enema administered by the patient in the hours prior to the exam maybe
 308 beneficial. However, an enema may also promote peristalsis, resulting in increased motion related
 309 artifacts in some instances. The patient should evacuate the rectum, if possible, just prior to the MRI exam.

| Parameter | Actor | Requirement |
|---------------------|--------------|------------------------------------------------------------------------------------------------------------------------------------------------------------------------------------------|
| Patient Positioning | Technologist | Serial study of each individual patient shall be performed on the same scanner using the same receiver coil and same positioning procedure (e.g. always head-first or always feet-first) |

310

311 **3.6. Image Data Acquisition**

312 This activity describes details of the data acquisition process that are necessary to reliably meet the Profile
 313 Claim. It may also include calibrations, performance assessments or validations during acquisition that
 314 are necessary to reliably meet the Profile Claim.

315 3.6.1 DISCUSSION

316 Tables in section 3.6.2 contain key specifications expressed using generic terminology. The specifications
 317 are consistent with publications supporting Profile Claims and consensus recommendations for brain [31,
 318 42-44, 67], liver [21, 28, 45-48, 55] and prostate [49-52, 54]. (Appendix D tabulates a standardized DWI
 319 phantom scanning protocol in vendor-specific terms that may be useful to harmonize patient DWI
 320 protocol across platforms [68-71].) Some parameters include a numerical range, and some requirements
 321 include qualifiers “acceptable” (base level to meet the claim), “target” (typical or default level to meet the
 322 claim), and “ideal” (expected higher performance available on some systems). Reduction of respiratory
 323 artifact in the liver requires either short breath-hold (un-averaged, <25 sec), or long (3-5 min) respiratory-
 324 synchronization, or free breathing with high signal averaging. The gain in image quality with high signal
 325 averaging favors use of non-breath-hold abdominal DWI. Section 4 and Appendix E describe DWI-specific
 326 (phantom-based) assessment procedures to ensure sufficient control of technical variability in DWI image
 327 acquisition to achieve the current Profile claims [68-75]. New techniques, such as simultaneous multi-
 328 slice or multi-band MRI, are becoming commercially available and could be advantageous for DWI [76-
 329 79]. However, these are not yet considered “standard” on most clinical systems and therefore are not
 330 specified below.

331 3.6.2 SPECIFICATION

332 The same acquisition methods repeated on the same scanner using parameter settings tabulated below
 333 are necessary to reliably meet the Profile Claim. DWI scan protocols shall be built by the MR technologist
 334 and/or MR physicist/scientist, clearly labeled and stored on the MRI system for recall in repeatable serial
 335 scan of patients. Version control of edits to the protocol should be tracked with prior versions archived.
 336

337
338

BRAIN

| Parameter | Actor | Requirement | DICOM Tag |
|------------------------------------------|---------------------------------------|----------------------------------------------------------------------|--------------|
| Field Strength | | 1.5 or 3T | [0018, 0087] |
| Acquisition sequence | | Diffusion-weighted Single-Shot Echo Planar Imaging (SS-EPI) | [0018, 0020] |
| Receive Coil type | | Ideal: 32 channel head array coil | [0018, 1250] |
| | | Target: 8-32 channel head array coil | |
| | | Acceptable: 8 channel head array coil | |
| Lipid suppression | | On | |
| Number of <i>b</i> -values | | Ideal: ≥ 3 (including one $b=0$) | |
| | | Acceptable/Target: 2 (including $b=0$) | |
| Minimum highest <i>b</i> -value strength | MR technologist /Physicist/ Scientist | Target/Ideal: $b=1000 \text{ s/mm}^2$ | [0018, 9087] |
| | | Acceptable: $b=850-999 \text{ s/mm}^2$ | |
| Diffusion directions | | Target/Ideal: ≥ 3 -orthogonal, combined gradient channels | [0018, 9075] |
| | | Acceptable: ≥ 3 -orthogonal, single gradient channels | [0018, 9089] |
| Slice thickness | | Ideal: $\leq 4 \text{ mm}$ | [0018, 0050] |
| | | Target: 4-5 mm | |
| | | Acceptable: 5mm | |
| Gap thickness | | Target/Ideal: 0-1 mm Acceptable: 1-2 mm | [0018, 0088] |
| Field-of-view | | Ideal/Target/Acceptable: 220-240 mm FOV along both axes | [0018, 1100] |
| Acquisition matrix | | Target/Ideal: (160-256) x (160-256), or 1.5-1 mm in-plane resolution | [0018, 1310] |
| | | Acceptable: 128 x 128, or 1.7 mm in-plane resolution | |
| Plane orientation | | Transversal-axial | [0020, 0037] |
| Phase-encode/ frequency-encode direction | | Anterior-Posterior / Right-Left | [0018, 1312] |
| Number of averages | | Ideal/Target: ≥ 2 | [0018, 0083] |
| | | Acceptable: 1 | |

| | | | |
|-----------------------------------------------|--|--------------------------------------------------------------------------------------------------------------------|--------------|
| In-plane parallel imaging acceleration factor | | Ideal: 2-3 Acceptable/Target: 2 | [0018, 9069] |
| TR | | Ideal: > 5000 ms Acceptable/Target: 3000-5000 ms | [0018, 0080] |
| TE | | Ideal: <60ms Target: minimum TE Acceptable: <120 ms | [0018, 0081] |
| Receiver Bandwidth | | Ideal/Target: maximum possible in frequency encoding direction (minimum echo spacing) Acceptable:>1000 Hz/voxel | [0018, 0095] |

339
340

LIVER

| Parameter | Actor | Requirement | DICOM Tag |
|------------------------------------------|-----------------------------------------|-----------------------------------------------------------------------------------------------------------------------------------------|------------------------------|
| Field Strength | | 1.5 or 3 T | [0018, 0087] |
| Acquisition sequence | | Diffusion-weighted Single-Shot Echo Planar Imaging (SS-EPI) | [0018, 0020] |
| Receive Coil type | | Ideal: >16 channel torso array coil Target: >6-16 channel torso array coil Acceptable: 6 channel torso array coil | [0018, 1250] |
| Lipid suppression | | On | |
| Number of <i>b</i> -values | | Ideal: ≥ 3 (including one $b < 50-100$ s/mm ²) Acceptable/Target: 2 (including one $b < 50-100$ s/mm ²) | |
| Minimum highest <i>b</i> -value strength | MR technologist / Physicist / Scientist | Target/Ideal: $b=600-800$ s/mm ² Acceptable: 500 s/mm ² | [0018, 9087] |
| Diffusion directions | | Target/Ideal: 3-orthogonal, combined gradient channels Acceptable: 3-orthogonal, single gradient channels | [0018, 9075] [0018, 9089] |
| Slice thickness | | Ideal: <5 mm Target: 5-7 mm Acceptable: 7-9 mm | [0018, 0050] |
| Gap thickness | | Ideal: 0 mm Target: 1 mm Acceptable: >1-2 mm | [0018, 0088] |
| Field-of-view | | Ideal/Target/Acceptable: 300-450 mm | [0018, 1100] |
| Acquisition matrix | | Target/Ideal: (160-196) x (160-192), or 2.5-2 | |

| | | | |
|------------------------------------------------|--|---------------------------------------------------------------------------------------|--------------|
| | | mm in-plane Acceptable: 128 x 128, or 3-2.6 mm in-plane resolution | [0018, 1310] |
| Plane orientation | | Transversal-axial | [0020, 0037] |
| Phase-encode/ frequency-encode direction | | Anterior-Posterior / Right-Left | [0018, 1312] |
| Number of averages | | Ideal: > 4 | [0018, 0083] |
| | | Target: 4 | |
| | | Acceptable: 2-3 | |
| Parallel imaging factor | | Ideal: 2-3 | [0018, 9069] |
| | | Target/Acceptable: 2 | |
| TR | | Ideal/Target/Acceptable > 2000 ms | [0018, 0080] |
| TE | | Ideal: < 60 ms | [0018, 0081] |
| | | Target: minimum TE | |
| | | Acceptable: < 110 ms | |
| Receiver Bandwidth | | Ideal/Target: maximum possible in frequency encoding direction (minimum echo spacing) | [0018, 0095] |
| | | Acceptable: > 1000 Hz/voxel | |

341
342
343
344

PROSTATE

| Parameter | Actor | Requirement | DICOM Tag |
|------------------------------------------|-----------------------------------------|----------------------------------------------------------------------------------------------------------------------------------------------------|--------------|
| Field Strength | | 3 T | [0018, 0087] |
| Acquisition sequence | | Diffusion-weighted Single-Shot Echo Planar Imaging (SS-EPI) | [0018,0020] |
| Receive Coil type | | Ideal: >8 channel torso array coil Target: >8 channel torso array coil Acceptable: pelvic phased array coil/endorectal coil; body array coil | [0018,1250] |
| Lipid suppression | | On | |
| Number of <i>b</i> -values | MR technologist / Physicist / Scientist | Ideal: ≥ 3 (including one $b < 50-100$ s/mm ²) | [0018, 9087] |
| | | Acceptable/Target: 2 (including one $b < 50-100$ s/mm ²) | |
| Minimum highest <i>b</i> -value strength | | Ideal: $b = 1000-1500$ s/mm ² | [0018, 9087] |
| | | Target/Acceptable: 500-1000 s/mm ² | |
| Diffusion directions | | Target/Ideal: 3-orthogonal, combined | |

| | | |
|------------------------------------------------|---------------------------------------------------------------------------------------|------------------------------|
| | gradient channels Acceptable: 3-orthogonal, single gradient channels | [0018, 9075] [0018, 9089] |
| Slice thickness | Ideal: <3 mm | |
| | Target: 3-4 mm | [0018, 0050] |
| | Acceptable: 4-5 mm | |
| Gap thickness | Ideal: 0 mm | |
| | Target/Acceptable: 1 mm | [0018, 0088] |
| | | |
| Field-of-view | Ideal/Target/Acceptable: 240-260 mm | [0018, 1100] |
| Acquisition matrix | Target/Ideal/Acceptable: (224-128) x (224-128), or 1-2 mm in-plane | [0018, 1310] |
| Plane orientation | Transversal-axial | [0020, 0037] |
| Phase-encode/ frequency-encode direction | Anterior-Posterior / Right-Left | [0018, 1312] |
| Number of averages | Ideal: > 4 | |
| | Target: 4 | [0018, 0083] |
| | Acceptable:2-4 | |
| Parallel imaging factor | Ideal /Target/Acceptable: 2 | [0018, 9069] |
| TR | Ideal/Target/Acceptable> 2000 ms | [0018, 0080] |
| TE | Ideal: < 60 ms | |
| | Target: minimum TE | [0018, 0081] |
| | Acceptable: < 90 ms | |
| Receiver Bandwidth | Ideal/Target: maximum possible in frequency encoding direction (minimum echo spacing) | [0018, 0095] |
| | Acceptable: > 1000 Hz/voxel | |

347 **3.7. Image Data Reconstruction**

348 This activity describes criteria and procedures related to producing images from the acquired data that
 349 are necessary to reliably meet the Profile Claim.

350 3.7.1 DISCUSSION

351 At a minimum, three-orthogonal directional DWI are acquired and reconstructed individually for each
 352 imaged slice, then combined into a directionally-independent (i.e. isotropic or trace) DWI [80, 81].
 353 Diffusion weighted images may be interpolated to an image matrix greater than the acquired matrix.
 354 Trace DWI (e.g. geometric average of 3-orthogonal directional DWI at same *b*-value) shall be automatically
 355 generated on the scanner and retained for each non-zero *b*-value, whereas retention of directional DWI
 356 is optional. ADC maps are typically generated on the scanner using a mono-exponential model trace DWI
 357 vs *b*-value. Alternatively, full DWI sets (directional plus trace, or trace alone) at all *b*-values can be
 358 provided for off-line ADC map generation (via mono-exponential model) on an independent workstation
 359 or thin-client distributed application.

360 Eddy currents and/or subject motion may create spatial misalignment or distortion between the individual
 361 directional DWI, and across *b*-values [82-84]. Direct combination of misaligned directional DWI will lead
 362 to spatial blur in trace DWI and subsequent artifact in ADC maps [82-84]. Spatial registration of directional
 363 DWI and/or trace DWI across all *b*-values may be performed on the scanner or off-line to reduce blur and
 364 improve quality of trace DWI and ADC maps.

365 Perfusion is known to affect diffusion measurement (a positive bias) particularly in highly vascular tissues
 366 (e.g. kidney and liver) [85-90]. ADC values derived from DWI spanning low *b*-value (i.e. $b < 50s/mm^2$) and
 367 modest high *b*-value (i.e. $b < 500s/mm^2$) increase perfusion bias. For diffusion measurement in liver, ADC
 368 maps may be reconstructed from DWI spanning 50-100s/mm² up to 800-900s/mm² to mitigate perfusion
 369 bias while maintaining adequate sensitivity to diffusion contrast and SNR. The *b*-value range used for ADC
 370 map generation shall be recorded and reported. Perfusion bias in brain DWI is considered small and
 371 typically ignored. There is a small deviation from monoexponential decay (pseudodiffusion) at low *b*-
 372 values in prostate [91].

373 3.7.2 SPECIFICATION

| Parameter | Actor | Requirement |
|----------------------------------|---------------------------------------------|-------------------------------------------------------------------------------------------------------------------------------------------------------------------------------------------------------------------------------------------------------------------------------------------------------------------------------------------------------------------------------------------------------------------------|
| Trace DWI and ADC map generation | MR technologist / Physicist Scientist | Procedural steps for image reconstruction/ADC map generation shall be held constant for all subjects and time points including: image interpolation; image registration prior to combination into trace DWI and across <i>b</i> -values; selection of <i>b</i> -values and fit algorithm to estimate ADC. ADC shall be calculated using the mono-exponential model of DWI signal decay with increasing <i>b</i> -value. |

374

375

376 3.8. Image QA

377 This activity describes criteria and evaluations of the images that are necessary to reliably meet the Profile
378 Claim.

379 3.8.1 DISCUSSION

380 At the time of image acquisition and review, quality of DWI data shall be checked for the following issues.
381 Poor quality due to sources below may be grounds to reject individual datasets.

- 382 ● Low SNR – Diffusion weighting inherently reduces signal, although signal must remain adequately
383 above the noise floor to properly estimate ADC [92-94]. Low SNR at high b -values can bias ADC
384 estimates. Visualization of anatomical features in tissues of interest at all b -values is acceptable
385 evidence that SNR is adequate for ADC measurement.
- 386 ● Ghost/parallel imaging artifacts – Discrete ghosts from extraneous signal sources along phase-
387 encode direction can obscure tissue of interest leading to unpredictable ADC values [83, 95-98].
- 388 ● Severe spatial distortion – Some level of spatial distortion is inherent to SS-EPI, although distortion
389 can be severe near high susceptibility gradients in tissues or metallic objects; or due to poor
390 magnet homogeneity [83, 97]. Severe distortion can alter apparent size/shape/volume of tissues
391 of interest thereby confound ROI definition, as well as adversely affect ADC values. Co-registration
392 to high-resolution (non-EPI) T_2 -weighted image volume may reduce these distortions.
- 393 ● Eddy currents – Distinct eddy currents amplified by strong diffusion pulses on different gradient
394 channels lead to spatial misalignment across DWI directions and b -values, and manifest as spatial
395 blur on trace DWI and erroneous ADC values, particularly at the edges of anatomical features [83,
396 99]. Distortion correction and image registration to $b = 0$ image prior to calculation of trace DWI
397 and ADC maps may reduce these errors.
- 398 ● Fat suppression – Lipid exhibits extremely low diffusion, with fat spatially shifted on SS-EPI from
399 its true source (by several cm along the phase-encode direction) due to chemical shift [100-104].
400 Of note, scanner frequency drifting due to the heating from high duty cycle diffusion gradients
401 could cause unsatisfactory fat suppression in the later frames of a diffusion acquisition, if only
402 chemical shift saturation technique is used for fat suppression. In such case, alternative or
403 additional fat suppression techniques, e.g. gradient reversal, could help to mitigate residual fat
404 signal. Superposition of unsuppressed fat signal onto tissue of interest can invalidate ADC
405 assessment there by partial volume averaging.
- 406 ● Motion artifacts — While SS-EPI is effective at freezing most bulk motion, variability of motion over
407 DWI directions and b -values contribute to blur and erroneous signal attenuation. Motion artifact
408 is anticipated to be low in brain DWI for most subjects, although cardiac-induced pulsation can
409 confound ADC measurement in/near ventricles and large vessels and in the brainstem. Respiratory
410 and cardiac motion artifacts are more problematic in the liver, particularly the left-lobe and
411 superior right lobe [12, 28, 97, 105, 106]. Quiet steady breathing or respiratory synchronization
412 and additional signal averaging are used to mitigate motion artifact in abdominal DWI. Residual
413 motion artifact can be recognized as inconsistent location of anatomical targets across b -values
414 and DWI directions and/or spatial modulation unrelated to anatomical features on DWI/ADC maps.
415 Inspection of DWI/ADC on orthogonal multiplanar reformat images aids detection of this artifact.

416 3.8.2 SPECIFICATION

417

| Parameter | Actor | Requirement |
|-----------|-------------------------------------------------------|------------------------------------------------------------------------------------------------------------------|
| ADC | Radiologist / MR technologist / Physicist / Scientist | Shall confirm DWI and ADC maps conform to adequate quality specifically considering points listed above (3.8.1). |

418

419 **3.9. Image Distribution**

420 This activity describes criteria and procedures related to distributing, transferring and archiving images
421 and metadata that are necessary to reliably meet the Profile Claim.

422 3.9.1 DISCUSSION

423 Images are distributed via network using Digital Imaging and Communications in Medicine (DICOM)
424 transfer protocol as per standard local practice. At a minimum, trace DWI at each acquired *b*-value must
425 be archived in the local picture archiving and communication system (PACS). Additionally, individual
426 direction DWI and ADC maps (if generated on the scanner) should be archived. DICOM tags essential for
427 downstream review and diffusion analysis must be maintained including, pixel intensity scaling [107], *b*-
428 value, and DWI directionality vs trace. DWI DICOM tags that store this information currently vary among
429 vendors. DICOM Parametric Map object [108] should be considered for storage of ADC maps, as it provides
430 unambiguous encoding of the quantity, units, *b*-values used and derivation method used for ADC
431 calculation [109]. The use of DICOM Parametric Map can facilitate interoperable and standardized
432 description of the DWI analysis results. It is noted that this object type is a recent introduction to the
433 DICOM standard and is not widely adopted among the vendors [108, 109].

434 3.9.2 SPECIFICATION

435

| Parameter | Actor | Requirement |
|-----------------|-----------------------------------------|---------------------------------------------------------------------------------------------------------------------------------------------------------------------------------------|
| Trace DWI | | All trace DWI at each acquired <i>b</i> -value shall be stored in local PACS and distributed to image analysis workstation(s) |
| ADC maps | MR technologist / Physicist / Scientist | ADC maps generated on the MRI scanner shall be stored in local PACS and distributed to image analysis workstation(s). <i>b</i> -values used for ADC map generation shall be recorded. |
| Directional DWI | | If directional DWI were generated on the MRI scanner in DICOM format, these shall be stored in local PACS and distributed to image analysis workstation(s). |

436

437 **3.10. Image Analysis**

438 This activity describes criteria and procedures related to producing quantitative measurements from the
439 images that are necessary to reliably meet the Profile Claim.

440 General considerations

441 In addition to initial Image QA (section 3.8), the radiologist / image analyst should confirm MR exams are
442 complete with all anatomical and DWI series, as well as screen for artifacts on DWI/ADC. Severe artifact

443 may lead to incorrect ADC calculation and should be excluded from ROIs placed on tissues of interest.
444 ADC maps shall be generated using mono-exponential model of signal attenuation vs b -value over the
445 range specified in section 3.6.2. ADC maps used for image analysis must be “equivalent” to ADC maps
446 generated on the MRI system. That is, all software elements along the image handling/network chain
447 must appropriately deal with potential DICOM scaling of DWI and ADC pixel values [107], otherwise
448 quantitative content is lost. The difference(s) in mean ADC within replicate ROIs defined on the scanner
449 and analysis workstation(s) should be less than the ROI standard deviation of the ADC. If ADC maps used
450 for analysis are generated offline, correct DICOM pixel scaling should be confirmed using a phantom
451 having absolute known ADC value (see Appendix D and E) or a DWI DRO (<https://goo.gl/YYPGOW>).

452 3.10.1 DISCUSSION: ROI DEFINITION IN DWI IMAGING

453 The measurements should be similar to those performed in ordinary clinical conditions. Level and range
454 of slices with tissue/tumor of interest should be reasonably matched each time the measurements are
455 performed. The use of ancillary MR images (e.g. T_1 -weighted, T_2 -weighted, post-gadolinium) can aid lesion
456 identification prior to ROI placement [21, 57, 67]. Tissue or lesion ADC quantification requires manual
457 placement of an ROI in two or three-dimensions. When performing ROI placement, the user must decide
458 which sequences (DWI, ADC maps, T_2 -weighted, T_1 -weighted with gadolinium, etc.) will be used to guide
459 selection tissue to be assayed, but the actual placement of the ROIs shall be on the diffusion images.

460

461 Procedural steps to create and extract quantities from ROIs varies among software packages. At times,
462 histogram analysis of whole tumor ROIs may be preferable to allow for distinction between predominantly
463 solid and heterogeneous cystic/necrotic lesions. Analysis steps, derived metrics and analysis software
464 package shall be held constant for all subjects and serial time points.

465

466 **Recommendations for ROI placement are organ-specific.**

467 3.10.1.1 Brain

468 ROIs should be manually placed on axial images where the tissues of interest are adequately conspicuous
469 on the DWI and/or ADC maps, or identifiable guided by ancillary MR images. The size of the ROI should
470 be chosen by the radiologist, though should be defined on relatively homogenous regions and matched
471 to select the same lesion/tissue assayed on prior time points. Selected ROI size should be sufficient to
472 represent the targeted ADC statistics. Avoid contamination within the ROI from tissues such as CSF or
473 that may have high iron content, such as acute or chronic hemorrhagic areas that have anomalous ADC
474 values. The brain may also contain areas of large necrotic cysts and surgical cavities - these areas should
475 be avoided.

476

477 3.10.1.2 LIVER

478 For liver parenchyma evaluation, ROIs should be large enough to avoid ADC values being unduly
479 influenced by random image noise and/or under-sampled regional heterogeneity. ROI placement should
480 avoid large vessels or extraneous anomalous ADC tissue unrelated to target tissue of interest such as cysts
481 or hemangiomas. Comparison of DWI at $b=0$ having high SNR revealing both vessels and focal lesions, to
482 moderately low b (< 100 s/mm²) where vessels are suppressed can be useful to localize lesions. It is also
483 important when assessing the ADC of liver parenchyma to avoid the lateral segment of the left lobe, as
484 this area is subject to pulsatile effects from the heart, leading to bias in high ADC values.

485

486 For liver lesion evaluation, the image that best reveals the lesion at high conspicuity is recommended. In
487 most cases, the low b -value image will provide the best visualization of lesion location and margins.

488 However, low *b*-value images alone will not allow the reader to distinguish between benign and malignant
 489 lesions, and inspection of higher *b*-value images and/or the ADC map is recommended.

490
 491 For large liver lesions, special consideration must be given to lesion heterogeneity. Large malignant
 492 lesions of the liver may contain areas of central necrosis or cystic degeneration. Avoidance of these areas
 493 is recommended so that one is limiting the quantitative assay to areas of solid tissue/tumor. However,
 494 while avoidance of cystic or necrotic areas is desirable, tumor effects that are marked by developing
 495 necrosis may be underestimated if one ignores cystic areas post treatment.
 496

497 **3.10.1.3 PROSTATE**

498 ROIs should be manually placed on axial images by the radiologist where the tissues of interest are
 499 adequately conspicuous on the DWI and/or ADC maps, or identifiable guided by ancillary MR images.

500 **3.10.2 SPECIFICATION**

501

| Parameter | Actor | Requirement |
|-------------------|-----------------------------------------------|------------------------------------------------------------------------------------------------------------------------------------------------------------------------------------------------------------------------------------------------------------------------------------------------------------------------------------------------------------------------------------------------------------------------------------------------------------------------------------------------------------------------------------------------------------------------------------------------------------|
| ROI Determination | Radiologist / Image Analyst / Scientist | Shall segment the ROI consistently across time points using the same software / analysis package |
| Image Display | Image Analysis Tool | Acceptable / Target: Software shall allow operator-defined ROI analysis of DWI/ADC aided by inspection of ancillary MR contrasts Ideal: Above plus multi view-port display where DWI/ADC and ancillary MR contrasts from the same scan date are displayed side-by-side and geometrically linked per DICOM (e.g cursor; cross-hair; ROI; automatically replicated in all view-ports); images from different scan date(s) can be displayed side-by-side, though not necessarily geometrically linked; and ROIs/VOIs may include multiple noncontiguous areas on one slice and/or over multiple slices |
| ADC statistics | Image Analysis Tool | Acceptable/Target: Shall allow display and retention of ROI statistics in patient DICOM database. Statistics shall include: ADC mean, standard deviation, and ROI/VOI area/volume Ideal: Additional statistics for ADC maximum, minimum, explicit inclusion vs exclusion of “NaNs” or zero-valued pixels in statistics, ADC pixel histogram, and retention of the ROI/VOI as a DICOM segmentation object |

502

503 **3.11. Image Interpretation**

504 This activity describes criteria and procedures related to clinically interpreting the measurements and
 505 images that are necessary to reliably meet the Profile Claim.

506 **3.11.1 DISCUSSION**

507 Low ADC values suggest cellular dense tissue and potentially solid/viable tumor as opposed to elevated

508 ADC values in tumor necrosis and cystic spaces. The use of specific interpretation of ADC values will
509 depend on the clinical application, e.g., taking into account spontaneous tumor necrosis versus tumor
510 necrosis after effective therapy. Schema and properties of tissues to assay by ADC should be addressed
511 during the design phase of each study. For example, therapies targeted to induce cytotoxic change in
512 solid viable tumor [3, 19, 22, 38, 40] are candidate for ADC monitoring by ROI segmentation guided by
513 traditional MR indicators of solid viable tissue, namely: relatively hyperintense on high *b*-value DWI, low
514 ADC, and perfused on dynamic contrast-enhanced MRI. The anticipated timescale of early therapeutic
515 response and/or tumor progression must be considered in study design of MRI scan dates for application
516 of ADC as a prognostic marker.

517

518 **4. Assessment Procedures**

519 To conform to this Profile, participating staff, software and equipment (**Actors**) shall support each activity
520 assigned to them in Table 1.

521 To support an activity, the **Actor** shall conform to the requirements (indicated by “shall” language) listed
522 in the specifications table of the activity subsection in Section 3.

523 Although most of the requirements described in Section 3 can be assessed for conformance by direct
524 observation, some of the baseline quantitative DWI performance-oriented requirements cannot, in which
525 case the requirement will reference an assessment procedure in a subsection here in Section 4.

526 Formal claims of conformance by the organization responsible for an Actor shall be in the form of a
527 published QIBA Conformance Statement. Vendors publishing a QIBA Conformance Statement shall
528 provide a set of “Model-Specific Parameters” (as shown in Appendix D) describing how their product was
529 configured to achieve conformance for quantitative DWI acquisition and analysis. Vendors shall also
530 provide access or describe the characteristics of the test set used for conformance testing.

531 **4.1. Assessment Procedure: MRI Equipment Specifications and Performance**

532 Conformance with this Profile requires adherence of MRI equipment to U.S. federal regulations [110] or
533 analogous regulations outside of the U.S., MRI equipment performance standards outlined by the
534 American Association of Physicists in Medicine [56] and/or by the American College of Radiology* as well
535 as quality control benchmarks established by the scanner manufacturer for the specific model. These
536 assessment procedures include a technical performance evaluation of the MRI scanner by a qualified
537 medical physicist or MRI scientist at least annually. Evaluated parameters include: magnetic field
538 uniformity, patient-handling equipment, gradient and RF subsystems safety, calibration and performance
539 checks. Periodic MR quality control must monitor image uniformity, contrast, spatial resolution, signal-to-
540 noise and artifacts using specific test objects and procedures (e.g., ACR phantom and QA procedure). In
541 addition, preventive maintenance at appropriate regular intervals must be conducted and documented
542 by a qualified service engineer.

543 Gradient subsystems are *explicitly* calibrated to properly encode 3D space, and are *implicitly* calibrated to
544 also encode diffusion. Performance procedures indicated above assess spatial encoding quality, although
545 diffusion weighting performance requires additional tests detailed in Appendix E. Key quantitative DWI
546 performance metrics include: ADC bias at magnet isocenter, random error within ROI (precision), SNR at
547 each *b*-value, ADC dependence on *b*-value and ADC spatial dependence. To conform to this Profile, system
548 performance benchmarks for these metrics are provided in Appendix E to ensure negligible contribution
549 of technical errors to above defined confidence intervals measured for tissue. These benchmarks reflect
550 the baseline MRI equipment performance in clinical and clinical trial settings which produced the data
551 used to support the Claims of this Profile. To establish tighter confidence bounds for ADC metrics,
552 additional technical assessment procedures may be introduced according to specific clinical trial protocol.

553 *http://www.acr.org/~/media/ACR_No_Index/Documents/QCManual/2015_MR_QCManual_Book.pdf.

554 **4.2. Assessment Procedure: Technologist**

555 Radiologic technologists shall fulfill the qualifications required by the ACR MRI Accreditation Program** or
556 analogous non-U.S. accreditation programs for non-U.S. facilities. These include certification by the

557 American Registry of Radiologic Technologists (ARRT) or analogous non-U.S. certifying organization,
558 appropriate licensing, documented training and experience in performing MRI, and compliance with
559 certifying and licensing organization continuing education requirements. The technologist shall be
560 capable of building, performing, and saving QA and DWI acquisition protocols for their specific system to
561 be consistent with this Profile. The technologist must be capable to perform all image processing steps to
562 create ADC maps on the scanner, and to recognize when automatic “in-line” ADC maps are defective (e.g.
563 noise threshold set too high causing artefactual null ADC zones in tissues).

564 [**
565 http://www.acraccreditation.org/~media/ACRAccreditation/Documents/MRI/Requirements.pdf?la=en
566 n](http://www.acraccreditation.org/~media/ACRAccreditation/Documents/MRI/Requirements.pdf?la=en)

567 **4.3. Assessment Procedure: Radiologists**

568 Radiologists shall fulfill the qualifications required by the ACR MRI Accreditation Program^{***} or analogous
569 non-U.S. accreditation programs for non-U.S. facilities. These include certification by the American Board
570 of Radiology or analogous non-U.S. certifying organization; appropriate licensing; documented oversight,
571 interpretation, and reporting of the required ABR minimum number of MRI examinations; and compliance
572 with ABR and licensing board continuing education requirements. Diffusion MRI does not specifically
573 require additional certification of the radiologist.

574 [***
575 http://www.acraccreditation.org/~media/ACRAccreditation/Documents/MRI/Requirements.pdf?la=en
576 n
577](http://www.acraccreditation.org/~media/ACRAccreditation/Documents/MRI/Requirements.pdf?la=en)

578 **4.4. Assessment Procedure: Image Analyst / Physicist / Scientist**

579 In clinical practice, it is expected that the radiologist interpreting the examination often will be the image
580 analyst. In some clinical practice situations, and in the clinical research setting, the image analyst may be
581 a non-radiologist professional such as a medical physicist, biomedical engineer, MRI scientist or 3D lab
582 technician. While there are currently no specific certification guidelines for image analysts, a non-
583 radiologist performing diffusion analysis shall be trained in technical aspects of DWI including:
584 understanding key acquisition principles of diffusion weighting and directionality and diffusion test
585 procedures (Appendix E); procedures to confirm that diffusion-related DICOM metadata content is
586 maintained along the network chain from scanner to PACS and analysis workstation. The analyst must be
587 expert in use of the image analysis software environment, including ADC map generation from DWI (if not
588 generated on the scanner), and ADC map reduction to statistics with ROI/VOI location(s) retained. The
589 analyst shall undergo documented training by a radiologist having qualifications conforming to the
590 requirements of this profile in terms of anatomical location and image contrast(s) used to select
591 measurement target. The level of training should be appropriate for the setting and the purpose of the
592 measurements, and may include instruction in topics such as directional and isotropic DWI and ADC map
593 reconstruction and processing; normative ADC values for select tissues; and recognition of image artifacts.
594

595 **4.5. Assessment Procedure: Image Analysis Software**

596 Often ADC maps are generated on the MRI system and distributed to the analysis workstation along with
597 source DWI and other available anatomical series. The image analyst / scientist must confirm ADC values
598 generated and measured on the scanner (e.g. mean ADC over a 1cm circular ROI) are equivalent to

599 replicate ROI values defined on scanner-generated ADC maps using intended analysis software. The level
600 of “equivalence” should be well within the ROI standard deviation. Discrepancy comparable to or greater
601 than the standard deviation suggests erroneous scaling of the ADC map by the image analysis software,
602 possibly due to incorrect or missing DICOM information. Any such discrepancy must be resolved before
603 proceeding with statistical analysis for profile compliance. Absolute image scaling and units of analysis
604 software-generated ADC maps must be available and stored in public DICOM tags such as
605 RealWorldValueMapping [0040,9096], RescaleIntercept [0028,1052], RescaleSlope [0028,1053] and
606 RescaleType [0028,1054] such that ADC map values are properly interpretable (e.g. “A true diffusion
607 coefficient of $1.1 \times 10^{-3} \text{ mm}^2/\text{s}$ is represented by an ADC map pixel/ROI value on the analysis workstation
608 as 1100.”). The use of the DICOM Parametric Map object [108, 109] can eliminate these discrepancies, as
609 it allows for storage of floating point voxel values. It also provides unambiguous encoding of the quantity,
610 units, b -values used and derivation method used for ADC calculation [109]. Image analysis software
611 vendors should consider the use of this object for storage of ADC maps.
612

613 When the image analysis software is used to generate ADC maps from source DWI, the software must use
614 a mono exponential model of DWI signal versus b -value. The DWI used to derive ADC maps shall be
615 “directionally-independent” (i.e. isotropic or trace DWI). If used for ADC map generation, image analysis
616 software must be able to extract b -value and diffusion axis direction content from the DICOM header to
617 appropriately derive ADC maps. In the event directionally-independent DWIs are not available, at least
618 three-orthogonal axes DWI must be provided at each non-zero b -value so that DWI traces at each b -value
619 are calculable for subsequent ADC map generation within the analysis software. The numerical software
620 conformance and signal-to-noise sensitivity (bias and range linearity with respect to ground-truth ADC
621 values) can be tested over the range of b -values and tissue-like ADC using the DWI digital reference object
622 [56], available on the QIDW (<https://goo.gl/yYPGOW>).
623
624

625 **References**

- 626 1. Baehring, J.M. and R.K. Fulbright, *Diffusion-weighted MRI in neuro-oncology*. CNS Oncol, 2012.
627 **1(2)**: p. 155-67.
- 628 2. Barboriak, D.P., *Imaging of brain tumors with diffusion-weighted and diffusion tensor MR*
629 *imaging*. Magn Reson Imaging Clin N Am, 2003. **11(3)**: p. 379-401.
- 630 3. Chenevert, T.L., et al., *Diffusion MRI: a new strategy for assessment of cancer therapeutic*
631 *efficacy*. Mol Imaging, 2002. **1(4)**: p. 336-43.
- 632 4. deSouza, N.M., A. Rockall, and S. Freeman, *Functional MR Imaging in Gynecologic Cancer*. Magn
633 Reson Imaging Clin N Am, 2016. **24(1)**: p. 205-22.
- 634 5. Galban, S., et al., *Diffusion-weighted MRI for assessment of early cancer treatment response*. Curr
635 Pharm Biotechnol, 2010. **11(6)**: p. 701-8.
- 636 6. Gao, X., et al., *Magnetic resonance imaging in assessment of treatment response of gamma knife*
637 *for brain tumors*. Chin Med J (Engl), 2011. **124(12)**: p. 1906-10.
- 638 7. Garcia-Figueiras, R., A.R. Padhani, and S. Baleato-Gonzalez, *Therapy Monitoring with Functional*
639 *and Molecular MR Imaging*. Magn Reson Imaging Clin N Am, 2016. **24(1)**: p. 261-88.
- 640 8. Higano, S., et al., *Malignant astrocytic tumors: clinical importance of apparent diffusion*
641 *coefficient in prediction of grade and prognosis*. Radiology, 2006. **241(3)**: p. 839-46.
- 642 9. Kang, Y., et al., *Gliomas: Histogram analysis of apparent diffusion coefficient maps with standard-*
643 *or high-b-value diffusion-weighted MR imaging--correlation with tumor grade*. Radiology, 2011.
644 **261(3)**: p. 882-90.
- 645 10. Kim, M. and H.S. Kim, *Emerging Techniques in Brain Tumor Imaging: What Radiologists Need to*
646 *Know*. Korean J Radiol, 2016. **17(5)**: p. 598-619.
- 647 11. Kim, S., et al., *Diffusion-weighted magnetic resonance imaging for predicting and detecting early*
648 *response to chemoradiation therapy of squamous cell carcinomas of the head and neck*. Clin
649 Cancer Res, 2009. **15(3)**: p. 986-94.
- 650 12. Koh, D.M., et al., *Body Diffusion-weighted MR Imaging in Oncology: Imaging at 3 T*. Magn Reson
651 Imaging Clin N Am, 2016. **24(1)**: p. 31-44.
- 652 13. Lupo, J.M. and S.J. Nelson, *Advanced magnetic resonance imaging methods for planning and*
653 *monitoring radiation therapy in patients with high-grade glioma*. Semin Radiat Oncol, 2014.
654 **24(4)**: p. 248-58.
- 655 14. Maier, S.E., Y. Sun, and R.V. Mulkern, *Diffusion imaging of brain tumors*. NMR Biomed, 2010.
656 **23(7)**: p. 849-64.
- 657 15. Murakami, R., et al., *Grading astrocytic tumors by using apparent diffusion coefficient*
658 *parameters: superiority of a one- versus two-parameter pilot method*. Radiology, 2009. **251(3)**: p.
659 838-45.
- 660 16. Nelson, S.J., *Assessment of therapeutic response and treatment planning for brain tumors using*
661 *metabolic and physiological MRI*. NMR Biomed, 2011. **24(6)**: p. 734-49.
- 662 17. Padhani, A.R., *Diffusion magnetic resonance imaging in cancer patient management*. Semin
663 Radiat Oncol, 2011. **21(2)**: p. 119-40.
- 664 18. Padhani, A.R. and A. Gogbashian, *Bony metastases: assessing response to therapy with whole-*
665 *body diffusion MRI*. Cancer Imaging, 2011. **11 Spec No A**: p. S129-45.
- 666 19. Padhani, A.R. and D.M. Koh, *Diffusion MR imaging for monitoring of treatment response*. Magn
667 Reson Imaging Clin N Am, 2011. **19(1)**: p. 181-209.
- 668 20. Padhani, A.R., D.M. Koh, and D.J. Collins, *Whole-body diffusion-weighted MR imaging in cancer:*
669 *current status and research directions*. Radiology, 2011. **261(3)**: p. 700-18.

- 670 21. Padhani, A.R., et al., *Diffusion-weighted magnetic resonance imaging as a cancer biomarker:*
671 *consensus and recommendations*. Neoplasia, 2009. **11**(2): p. 102-25.
- 672 22. Patterson, D.M., A.R. Padhani, and D.J. Collins, *Technology insight: water diffusion MRI--a*
673 *potential new biomarker of response to cancer therapy*. Nat Clin Pract Oncol, 2008. **5**(4): p. 220-
674 33.
- 675 23. Pope, W.B., et al., *Recurrent glioblastoma multiforme: ADC histogram analysis predicts response*
676 *to bevacizumab treatment*. Radiology, 2009. **252**(1): p. 182-9.
- 677 24. Provenzale, J.M., S. Mukundan, and D.P. Barboriak, *Diffusion-weighted and perfusion MR*
678 *imaging for brain tumor characterization and assessment of treatment response*. Radiology,
679 2006. **239**(3): p. 632-49.
- 680 25. Rosenkrantz, A.B., et al., *Body diffusion kurtosis imaging: Basic principles, applications, and*
681 *considerations for clinical practice*. J Magn Reson Imaging, 2015. **42**(5): p. 1190-202.
- 682 26. Schmainda, K.M., *Diffusion-weighted MRI as a biomarker for treatment response in glioma*. CNS
683 Oncol, 2012. **1**(2): p. 169-80.
- 684 27. Shiroishi, M.S., J.L. Boxerman, and W.B. Pope, *Physiologic MRI for assessment of response to*
685 *therapy and prognosis in glioblastoma*. Neuro Oncol, 2016. **18**(4): p. 467-78.
- 686 28. Taouli, B. and D.M. Koh, *Diffusion-weighted MR imaging of the liver*. Radiology, 2010. **254**(1): p.
687 47-66.
- 688 29. Yamasaki, F., et al., *Apparent diffusion coefficient of human brain tumors at MR imaging*.
689 Radiology, 2005. **235**(3): p. 985-91.
- 690 30. Barnhart, H.X. and D.P. Barboriak, *Applications of the repeatability of quantitative imaging*
691 *biomarkers: a review of statistical analysis of repeat data sets*. Transl Oncol, 2009. **2**(4): p. 231-5.
- 692 31. Goldmacher, G.V., et al., *Standardized Brain Tumor Imaging Protocol for Clinical Trials*. AJNR Am J
693 Neuroradiol, 2015. **36**(10): p. E65-6.
- 694 32. Jackson, E.F., et al., *Magnetic resonance assessment of response to therapy: tumor change*
695 *measurement, truth data and error sources*. Transl Oncol, 2009. **2**(4): p. 211-5.
- 696 33. Meyer, C.R., et al., *Quantitative imaging to assess tumor response to therapy: common themes of*
697 *measurement, truth data, and error sources*. Transl Oncol, 2009. **2**(4): p. 198-210.
- 698 34. Obuchowski, N.A., et al., *Statistical Issues in Testing Conformance with the Quantitative Imaging*
699 *Biomarker Alliance (QIBA) Profile Claims*. Acad Radiol, 2016. **23**(4): p. 496-506.
- 700 35. Obuchowski, N.A., et al., *Quantitative imaging biomarkers: a review of statistical methods for*
701 *computer algorithm comparisons*. Stat Methods Med Res, 2015. **24**(1): p. 68-106.
- 702 36. Raunig, D.L., et al., *Quantitative imaging biomarkers: a review of statistical methods for technical*
703 *performance assessment*. Stat Methods Med Res, 2015. **24**(1): p. 27-67.
- 704 37. Sullivan, D.C., et al., *Metrology Standards for Quantitative Imaging Biomarkers*. Radiology, 2015.
705 **277**(3): p. 813-25.
- 706 38. Li, S.P. and A.R. Padhani, *Tumor response assessments with diffusion and perfusion MRI*. J Magn
707 Reson Imaging, 2012. **35**(4): p. 745-63.
- 708 39. O'Connor, J.P., et al., *Imaging biomarker roadmap for cancer studies*. Nat Rev Clin Oncol, 2016.
- 709 40. Chenevert, T.L., P.C. Sundgren, and B.D. Ross, *Diffusion imaging: insight to cell status and*
710 *cytoarchitecture*. Neuroimaging Clin N Am, 2006. **16**(4): p. 619-32, viii-ix.
- 711 41. Ross, B.D., et al., *Evaluation of cancer therapy using diffusion magnetic resonance imaging*. Mol
712 Cancer Ther, 2003. **2**(6): p. 581-7.
- 713 42. Bonekamp, D., et al., *Diffusion tensor imaging in children and adolescents: reproducibility,*
714 *hemispheric, and age-related differences*. Neuroimage, 2007. **34**(2): p. 733-42.
- 715 43. Paldino, M.J., et al., *Repeatability of quantitative parameters derived from diffusion tensor*

- 716 *imaging in patients with glioblastoma multiforme*. J Magn Reson Imaging, 2009. **29**(5): p. 1199-
717 205.
- 718 44. Pfefferbaum, A., E. Adalsteinsson, and E.V. Sullivan, *Replicability of diffusion tensor imaging*
719 *measurements of fractional anisotropy and trace in brain*. J Magn Reson Imaging, 2003. **18**(4): p.
720 427-33.
- 721 45. Braithwaite, A.C., et al., *Short- and midterm reproducibility of apparent diffusion coefficient*
722 *measurements at 3.0-T diffusion-weighted imaging of the abdomen*. Radiology, 2009. **250**(2): p.
723 459-65.
- 724 46. Deckers, F., et al., *Apparent diffusion coefficient measurements as very early predictive markers*
725 *of response to chemotherapy in hepatic metastasis: a preliminary investigation of reproducibility*
726 *and diagnostic value*. J Magn Reson Imaging, 2014. **40**(2): p. 448-56.
- 727 47. Heijmen, L., et al., *Diffusion-weighted MR imaging in liver metastases of colorectal cancer:*
728 *reproducibility and biological validation*. Eur Radiol, 2013. **23**(3): p. 748-56.
- 729 48. Miquel, M.E., et al., *In vitro and in vivo repeatability of abdominal diffusion-weighted MRI*. Br J
730 Radiol, 2012. **85**(1019): p. 1507-12.
- 731 49. Gibbs, P., Pickles, M.D., L.W. Turnbull, *Repeatability of echo-planar-based diffusion*
732 *measurements of the human prostate at 3T*. Magn Reson Imaging, 2007. **25**(10): p. 1423-9.
- 733 50. Jambor, I., et al., *Optimization of b-value distribution for biexponential diffusion-weighted MR*
734 *imaging of normal prostate*. J Magn Reson Imaging, 2014. **39**(5): p. 1213-22.
- 735 51. Jambor, I., et al., *Evaluation of different mathematical models for diffusion-weighted imaging of*
736 *normal prostate and prostate cancer using high b-values: a repeatability study*. Magn Reson Med,
737 2015. **73**(5): p. 1988-98.
- 738 52. Litjens, G.J., et al., *Interpatient variation in normal peripheral zone apparent diffusion coefficient:*
739 *effect on the prediction of prostate cancer aggressiveness*. Radiology, 2012. **265**(1): p. 260-6.
- 740 53. Afaq, A., et al., *Clinical utility of diffusion-weighted magnetic resonance imaging in prostate*
741 *cancer*. BJU Int, 2011. **108**(11): p. 1716-22.
- 742 54. Fedorov, A., et al., *Multiparametric MRI of the prostate: repeatability of volume and apparent*
743 *diffusion coefficient quantification*. Invest Radiol, 2017. **(in press)**.
- 744 55. Winfield, J.M., et al., *Extracranial Soft-Tissue Tumors: Repeatability of Apparent Diffusion*
745 *Coefficient Estimates from Diffusion-weighted MR Imaging*. Radiology, 2017: p. 161965.
- 746 56. Jackson, E.F., et al. *Acceptance Testing and Quality Assurance Procedures for Magnetic*
747 *Resonance Imaging Facilities*
748 *Report of MR Subcommittee Task Group I*. 2010; Available from:
749 http://www.aapm.org/pubs/reports/RPT_100.pdf.
- 750 57. Ellingson, B.M., et al., *Diffusion MRI quality control and functional diffusion map results in ACRIN*
751 *6677/RTOG 0625: a multicenter, randomized, phase II trial of bevacizumab and chemotherapy in*
752 *recurrent glioblastoma*. Int J Oncol, 2015. **46**(5): p. 1883-92.
- 753 58. Shellock, F.G. and J.V. Cruess, *MR procedures: biologic effects, safety, and patient care*. Radiology,
754 2004. **232**(3): p. 635-52.
- 755 59. Shellock, F.G. and A. Spinazzi, *MRI safety update 2008: part 2, screening patients for MRI*. AJR Am
756 J Roentgenol, 2008. **191**(4): p. 1140-9.
- 757 60. Shellock, F.G. and A. Spinazzi, *MRI safety update 2008: part 1, MRI contrast agents and*
758 *nephrogenic systemic fibrosis*. AJR Am J Roentgenol, 2008. **191**(4): p. 1129-39.
- 759 61. Shinbane, J.S., P.M. Colletti, and F.G. Shellock, *Magnetic resonance imaging in patients with*
760 *cardiac pacemakers: era of "MR Conditional" designs*. J Cardiovasc Magn Reson, 2011. **13**: p. 63.
- 761 62. Ciet, P. and D.E. Litmanovich, *MR safety issues particular to women*. Magn Reson Imaging Clin N

- 762 Am, 2015. **23**(1): p. 59-67.
- 763 63. Enders, J., et al., *Reduction of claustrophobia during magnetic resonance imaging: methods and*
764 *design of the "CLAUSTRO" randomized controlled trial.* BMC Med Imaging, 2011. **11**: p. 4.
- 765 64. Tee, L.M., et al., *Magnetic resonance imaging of the fetal brain.* Hong Kong Med J, 2016. **22**(3): p.
766 270-8.
- 767 65. Tsai, L.L., et al., *A Practical Guide to MR Imaging Safety: What Radiologists Need to Know.*
768 Radiographics, 2015. **35**(6): p. 1722-37.
- 769 66. Calamante, F., et al., *MR system operator: recommended minimum requirements for performing*
770 *MRI in human subjects in a research setting.* J Magn Reson Imaging, 2015. **41**(4): p. 899-902.
- 771 67. Ellingson, B.M., et al., *Consensus recommendations for a standardized Brain Tumor Imaging*
772 *Protocol in clinical trials.* Neuro Oncol, 2015. **17**(9): p. 1188-98.
- 773 68. Chenevert, T.L., et al., *Diffusion coefficient measurement using a temperature-controlled fluid for*
774 *quality control in multicenter studies.* J Magn Reson Imaging, 2011. **34**(4): p. 983-7.
- 775 69. Jerome, N.P., et al., *Development of a temperature-controlled phantom for magnetic resonance*
776 *quality assurance of diffusion, dynamic, and relaxometry measurements.* Med Phys, 2016. **43**(6):
777 p. 2998.
- 778 70. Malyarenko, D., et al., *Multi-system repeatability and reproducibility of apparent diffusion*
779 *coefficient measurement using an ice-water phantom.* J Magn Reson Imaging, 2013. **37**(5): p.
780 1238-46.
- 781 71. Mulkern, R.V., et al., *Pediatric brain tumor consortium multisite assessment of apparent diffusion*
782 *coefficient z-axis variation assessed with an ice-water phantom.* Acad Radiol, 2015. **22**(3): p. 363-
783 9.
- 784 72. Malkyarenko, D.I. and T.L. Chenevert, *Practical estimate of gradient nonlinearity for*
785 *implementation of apparent diffusion coefficient bias correction.* J Magn Reson Imaging, 2014.
786 **40**(6): p. 1487-95.
- 787 73. Malyarenko, D.I., et al., *Demonstration of nonlinearity bias in the measurement of the apparent*
788 *diffusion coefficient in multicenter trials.* Magn Reson Med, 2016. **75**(3): p. 1312-23.
- 789 74. Malyarenko, D.I., et al., *Correction of Gradient Nonlinearity Bias in Quantitative Diffusion*
790 *Parameters of Renal Tissue with Intra Voxel Incoherent Motion.* Tomography, 2015. **1**(2): p. 145-
791 151.
- 792 75. Malyarenko, D.I., B.D. Ross, and T.L. Chenevert, *Analysis and correction of gradient nonlinearity*
793 *bias in apparent diffusion coefficient measurements.* Magn Reson Med, 2014. **71**(3): p. 1312-23.
- 794 76. Barth, M., et al., *Simultaneous multislice (SMS) imaging techniques.* Magn Reson Med, 2016.
795 **75**(1): p. 63-81.
- 796 77. Eichner, C., et al., *Slice accelerated diffusion-weighted imaging at ultra-high field strength.* Magn
797 Reson Med, 2014. **71**(4): p. 1518-25.
- 798 78. Obele, C.C., et al., *Simultaneous Multislice Accelerated Free-Breathing Diffusion-Weighted*
799 *Imaging of the Liver at 3T.* Abdom Imaging, 2015. **40**(7): p. 2323-30.
- 800 79. Wu, X., et al., *Simultaneous multislice multiband parallel radiofrequency excitation with*
801 *independent slice-specific transmit B1 homogenization.* Magn Reson Med, 2013. **70**(3): p. 630-8.
- 802 80. Sorensen, A.G., et al., *Hyperacute stroke: evaluation with combined multisection diffusion-*
803 *weighted and hemodynamically weighted echo-planar MR imaging.* Radiology, 1996. **199**(2): p.
804 391-401.
- 805 81. van Gelderen, P., et al., *Water diffusion and acute stroke.* Magn Reson Med, 1994. **31**(2): p. 154-
806 63.
- 807 82. Bastin, M.E., *Correction of eddy current-induced artefacts in diffusion tensor imaging using*

- 808 *iterative cross-correlation*. Magn Reson Imaging, 1999. **17**(7): p. 1011-24.
- 809 83. Le Bihan, D., et al., *Artifacts and pitfalls in diffusion MRI*. J Magn Reson Imaging, 2006. **24**(3): p.
810 478-88.
- 811 84. Mohammadi, S., et al., *Correcting eddy current and motion effects by affine whole-brain*
812 *registrations: evaluation of three-dimensional distortions and comparison with slice-wise*
813 *correction*. Magn Reson Med, 2010. **64**(4): p. 1047-56.
- 814 85. Dyvorne, H.A., et al., *Diffusion-weighted imaging of the liver with multiple b values: effect of*
815 *diffusion gradient polarity and breathing acquisition on image quality and intravoxel incoherent*
816 *motion parameters--a pilot study*. Radiology, 2013. **266**(3): p. 920-9.
- 817 86. Kakite, S., et al., *Hepatocellular carcinoma: short-term reproducibility of apparent diffusion*
818 *coefficient and intravoxel incoherent motion parameters at 3.0T*. J Magn Reson Imaging, 2015.
819 **41**(1): p. 149-56.
- 820 87. LeBihan, D., *IVIM method measures diffusion and perfusion*. Diagn Imaging (San Franc), 1990.
821 **12**(6): p. 133, 136.
- 822 88. Lee, Y., et al., *Intravoxel incoherent motion diffusion-weighted MR imaging of the liver: effect of*
823 *triggering methods on regional variability and measurement repeatability of quantitative*
824 *parameters*. Radiology, 2015. **274**(2): p. 405-15.
- 825 89. Takahara, T. and T.C. Kwee, *Low b-value diffusion-weighted imaging: emerging applications in*
826 *the body*. J Magn Reson Imaging, 2012. **35**(6): p. 1266-73.
- 827 90. Yoon, J.H., et al., *Evaluation of hepatic fibrosis using intravoxel incoherent motion in diffusion-*
828 *weighted liver MRI*. J Comput Assist Tomogr, 2014. **38**(1): p. 110-6.
- 829 91. Merisaari, H., et al., *Fitting methods for intravoxel incoherent motion imaging of prostate cancer*
830 *on region of interest level: Repeatability and gleason score prediction*. Magn Reson Med, 2017.
831 **77**(3): p. 1249-1264.
- 832 92. Basu, S., T. Fletcher, and R. Whitaker, *Rician noise removal in diffusion tensor MRI*. Med Image
833 Comput Comput Assist Interv, 2006. **9**(Pt 1): p. 117-25.
- 834 93. Kristoffersen, A., *Optimal estimation of the diffusion coefficient from non-averaged and averaged*
835 *noisy magnitude data*. J Magn Reson, 2007. **187**(2): p. 293-305.
- 836 94. Lui, D., et al., *Monte Carlo bias field correction in endorectal diffusion imaging*. IEEE Trans Biomed
837 Eng, 2014. **61**(2): p. 368-80.
- 838 95. Chen, N.K. and A.M. Wyrwicz, *Removal of EPI Nyquist ghost artifacts with two-dimensional phase*
839 *correction*. Magn Reson Med, 2004. **51**(6): p. 1247-53.
- 840 96. Guglielmo, F.F., et al., *Hepatic MR imaging techniques, optimization, and artifacts*. Magn Reson
841 Imaging Clin N Am, 2014. **22**(3): p. 263-82.
- 842 97. Koh, D.M., et al., *Whole-body diffusion-weighted MRI: tips, tricks, and pitfalls*. AJR Am J
843 Roentgenol, 2012. **199**(2): p. 252-62.
- 844 98. Kuhl, C.K., et al., *Sensitivity encoding for diffusion-weighted MR imaging at 3.0 T: intraindividual*
845 *comparative study*. Radiology, 2005. **234**(2): p. 517-26.
- 846 99. Reese, T.G., et al., *Reduction of eddy-current-induced distortion in diffusion MRI using a twice-*
847 *refocused spin echo*. Magn Reson Med, 2003. **49**(1): p. 177-82.
- 848 100. Bendel, P. and Y. Schiffenbauer, *A method for fat suppression in MRI based on diffusion-weighted*
849 *imaging*. Phys Med Biol, 2010. **55**(22): p. N547-55.
- 850 101. Hansmann, J., D. Hernando, and S.B. Reeder, *Fat confounds the observed apparent diffusion*
851 *coefficient in patients with hepatic steatosis*. Magn Reson Med, 2013. **69**(2): p. 545-52.
- 852 102. Hernando, D., et al., *Removal of olefinic fat chemical shift artifact in diffusion MRI*. Magn Reson
853 Med, 2011. **65**(3): p. 692-701.

- 854 103. Nagy, Z. and N. Weiskopf, *Efficient fat suppression by slice-selection gradient reversal in twice-*
855 *refocused diffusion encoding*. Magn Reson Med, 2008. **60**(5): p. 1256-60.
- 856 104. Sarlls, J.E., et al., *Robust fat suppression at 3T in high-resolution diffusion-weighted single-shot*
857 *echo-planar imaging of human brain*. Magn Reson Med, 2011. **66**(6): p. 1658-65.
- 858 105. Kwee, T.C., et al., *Diffusion-weighted whole-body imaging with background body signal*
859 *suppression (DWIBS): features and potential applications in oncology*. Eur Radiol, 2008. **18**(9): p.
860 1937-52.
- 861 106. Takahara, T., et al., *Diffusion-weighted magnetic resonance imaging of the liver using tracking*
862 *only navigator echo: feasibility study*. Invest Radiol, 2010. **45**(2): p. 57-63.
- 863 107. Chenevert, T.L., et al., *Errors in Quantitative Image Analysis due to Platform-Dependent Image*
864 *Scaling*. Transl Oncol, 2014. **7**(1): p. 65-71.
- 865 108. DICOM. *Parametric Map IOD Description*. Available from:
866 http://dicom.nema.org/medical/dicom/current/output/chtml/part03/sect_A.75.html.
- 867 109. NEMA. *ADCmodelparameters*. Available from:
868 ftp://medical.nema.org/medical/dicom/cp/cp1665_vp_ADCmodelparameters.pdf.
- 869 110. Delfino, J.G., *U.S. federal safety standards, guidelines and regulations for MRI systems: An*
870 *overview*. Applied Radiology, 2015: p. 20-23.
- 871 111. Boss, M.A., et al. *Temperature-Controlled Isotropic Diffusion Phantom with Wide Range of*
872 *Apparent Diffusion Coefficients for Multicenter Assessment of Scanner Repeatability and*
873 *Reproducibility*. in *Proceeding of the International Society of Magnetic Resonance in Medicine*.
874 2014. Milan, Italy.
- 875 112. Sijbers, J. and A.J. den Dekker, *Maximum likelihood estimation of signal amplitude and noise*
876 *variance from MR data*. Magn Reson Med, 2004. **51**(3): p. 586-94.
- 877 113. Friedman, L. and G.H. Glover, *Report on a multicenter fMRI quality assurance protocol*. J Magn
878 Reson Imaging, 2006. **23**(6): p. 827-39.
- 879 114. Bammer, R., et al., *Analysis and generalized correction of the effect of spatial gradient field*
880 *distortions in diffusion-weighted imaging*. Magn Reson Med, 2003. **50**(3): p. 560-9.
- 881
- 882

883
884

885 **Appendices**

886 **Appendix A: Acknowledgements and Attributions**

887 This document is proffered by the Radiological Society of North America [37], Diffusion-Weighted Imaging
888 Task Force subgroup of the Perfusion Diffusion and Flow (PDF) Biomarker Committee. The PDF is
889 composed of scientists, engineers, and clinicians representing academia, the imaging device
890 manufacturers, image analysis software developers, image analysis laboratories, biopharmaceutical
891 industry, government research organizations, professional societies, and regulatory agencies, among
892 others. All work is classified as pre-competitive.

893 The following individuals have made critical contributions in the development of this Profile:

| | |
|---------------------|---------------------|
| Rajpaul Attariwala | Chen Lin |
| Daniel Barboriak | Mikko Määttä |
| David Bennett | Dariya Malyarenko |
| Ishtiaq Bercha | Elizabeth Mirowski |
| Michael Boss | Bastien Moreau |
| Orest Boyko | Nancy Obuchowski |
| Martin Büchert | Estanislao Oubel |
| Thomas Chenevert | Savannah Partridge |
| Caroline Chung | Thorsten Persigehl |
| Amita Shukla Dave | Mark Rosen |
| Andrey Fedorov | Mark Shiroishi |
| Clifton Fuller | Rohit Sood |
| Alexander Guimaraes | Daniel Sullivan |
| Marko Ivancevic | Ying Tang |
| Edward Jackson | Bachir Taouli |
| Ivan Jambor | Aradhana Venkatesan |
| John Kirsch | Ona Wu |
| Daniel Krainak | Junqian Xu |
| Hendrik Laue | Gudrun Zahlmann |
| Jiachao Liang | |

894

895 We also acknowledge the extraordinary efforts by RSNA QIBA staff in making this Profile possible.

896

897 **Appendix B: Background Information**

898 QIBA Wiki:

899 http://qibawiki.rsna.org/index.php/Main_Page

900 QIBA Perfusion, Diffusion, and Flow Biomarker Committee Wiki:

901 <http://qibawiki.rsna.org/index.php/Perfusion, Diffusion and Flow-MRI Biomarker Ctte>

902 DWI Literature Review:

903 <http://qibawiki.rsna.org/index.php/DWI Literature Review>

904 QIBAPhan Analysis Software (for ADC and summary statistics of isotropic diffusion phantom):

905 <https://goo.gl/xjHc6G>

906 QIBA DWI Digital Reference Object:

907 <https://goo.gl/yYPGOW>

908 Diffusion Phantom Preparation and Positioning:

909 <http://qibawiki.rsna.org/index.php/Perfusion, Diffusion and Flow-MRI Biomarker Ctte>

910 DICOM MR Diffusion Macro:

911 http://dicom.nema.org/medical/dicom/current/output/chtml/part03/sect_C.8.13.5.9.html

912 **Appendix C: Conventions and Definitions**

913 **Apparent Diffusion Coefficient (ADC):** A quantitative imaging biomarker (typically in units mm^2/s or
914 $\mu\text{m}^2/\text{ms}$) indicative of the mobility of water molecules. High ADC indicates free or less hindered mobility
915 of water; low ADC indicates slow, restricted, or hindered mobility of water molecules.

916 ***b*-value:** An indication of the strength of diffusion-weighting (typically in units of s/mm^2). It depends on
917 a combination of gradient pulse duration, shape, strength, and the timing between diffusion gradient
918 pulses.

919 **DICOM:** Digital Imaging and Communications in Medicine standard for distributing and viewing any kind
920 of medical image regardless of the origin. A DWI DICOM header typically contains meta-data reflecting
921 scan geometry and key acquisition parameters (e.g., *b*-value and gradient direction) required for
922 subsequent generation of ADC maps and ROI statistics. A DWI DICOM macro assigns the required
923 diffusion-specific attributes to public DICOM tags ([0018, 9087] & [0018, 9098]) which should be
924 available independent of Vendor and scanner software version. Currently, vendors do not universally
925 follow the DWI macro standard, storing *b*-value and direction metadata in private tags.

926 **Diffusion Weighted Image (DWI):** A type of MR image where tissue contrast is dependent on water
927 mobility, diffusion gradient direction, concentration of water signal, and T_2 relaxation. On heavily
928 diffusion-weighted images (i.e. high *b*-value), high signal indicates low water mobility, high proton
929 concentration, and/or long T_2 .

930 **Isotropic (or trace) DWI:** Directionally-independent diffusion-weighted images obtained as the
931 composite (geometric average) of three orthogonal DWIs and used for ADC map derivation. Throughout
932 this profile and assessment procedure, the term “DWI” refers to these directionally-independent images
933 unless otherwise noted as a specific single-axis or directional DWI. Even in anisotropic media,
934 directionally-independent (i.e. scalar) diffusion metrics are measurable using DWI combined from three-
935 orthogonal diffusion gradient acquisitions.

936 **Repeatability Coefficient (RC):** Represents measurement precision where conditions of the

937 measurement procedure (scanner, acquisition parameters, slice locations, image reconstruction,
 938 operator, and analysis) are held constant over a “short interval”.

939 **Within-subject Coefficient of Variance (wCV):** Is often reported for repeatability studies to assess
 940 repeatability in test–retest designs. Calculated as seen in the table below:

941 **Steps for Calculating the wCV**

| | |
|---|----------------------------------------------------------------------------------------------------|
| 1 | Calculate the variance and mean for each of N subjects from their replicate measurements. |
| 2 | Calculate the wCV^2 for each of the N subjects by dividing their variance by their mean squared. |
| 3 | Take the mean of the wCV^2 over the N subjects. |
| 4 | Take the square root of the value in step 3 to get an estimate of the wCV. |

942

943 **Appendix D: Platform-Specific Acquisition Parameters for DWI Phantom Scans**

944 For acquisition modalities, reconstruction software and software analysis tools, profile conformance
 945 requires meeting the activity specifications and assessment requirements above in Sections 2, 3 and 4.

946 This Appendix provides specific acquisition parameters, reconstruction parameters and analysis software
 947 parameters that are expected to achieve compatibility with profile requirements for technical assessment
 948 of MRI systems. Just using these parameters without meeting the requirements specified in the profile
 949 is not sufficient to achieve conformance. Conversely, it is possible to use different compatible parameters
 950 and still achieve conformance. System operation within provided conformance limits suggests the
 951 technical contribution to variance does not unduly alter wCV observed in biological measurements.
 952 Technical DWI performance of a given MRI system relative to peer systems can be assessed using the
 953 described standardized acquisition protocols designed for existing ice-water DWI phantoms. Platform-
 954 specific protocols were excerpted from the QIBA ice water-based DWI Phantom scan procedure for axial
 955 acquisitions. The full QIBA DWI Phantom scan procedure involves acquisitions for coronal, axial and
 956 sagittal planes as detailed in the QIBA DWI wiki.

957 Sites using MRI system models listed here are encouraged to consider using parameter settings provided
 958 in this Profile for both simplicity and consistency of periodic quantitative DWI QA procedures. Sites using
 959 models not listed here may be able to devise their own settings that result in data meeting the
 960 requirements of this Profile (at the minimum) or tighter requirements of specific clinical trial.

961 **IMPORTANT: The presence of a product model/version in these tables does not imply it has**
 962 **demonstrated conformance with the QIBA Profile. Refer to the QIBA Conformance Statement for the**
 963 **product.**

964

965

966

967

Table D.1 Model-specific Parameters for Acquisition Devices When Scanning DWI Phantoms

| Acquisition Device | Settings Compatible with Conformance | | |
|-------------------------|----------------------------------------------------------------------|---------------------------------|------------------------------------|
| Philips | <i>Submitted by: University of Michigan, Department of Radiology</i> | | |
| | Model / Version | Achieva / 5.1.7 | Ingenia / 5.1.7 |
| | Field Strength | 1.5T | 3T |
| | Receiver Coil | ≥8ch head | ≥ 15ch head |
| | Uniformity | CLEAR=yes; Body-Tuned=no | CLEAR = yes |
| | Slice Orientation | Transaxial | Transaxial |
| | FOV | 220mm | 220mm |
| | Acquisition Voxel Size | 1.72x1.72x4mm | 1.72x1.72x4mm |
| | Acquisition Matrix | 128x126 | 128x128 |
| | Recon Voxel Size | 0.898x0.898x4mm | 0.898x0.898x4mm |
| | Recon Matrix | 256x256 | 256x256 |
| | SENSE (parallel imaging) | Yes, factor=2 | Yes, factor=2 |
| | Fold-over Direction | AP | AP |
| | Fat-shift direction | P | P |
| | Foldover-sup / Oversampling | No | No |
| | Qty Slices | 25 | 25 |
| | Stacks and Packages | 1 | 1 |
| | Slice Thickness | 4mm | 4mm |
| | Slice gap (user-defined) | 1mm | 1mm |
| | Shim | Volume set to encompass phantom | Vol or PB-Vol to encompass phantom |
| | B1 shim | Not Applicable | Fixed |
| | Scan Mode | MS | MS |
| | Technique | SE | SE |
| | Acquisition Mode | Cartesian | Cartesian |
| | Fast Imaging Mode | EPI | EPI |
| | Shot Mode | Single-shot | Single-shot |
| | Echoes | 1 | 1 |
| | Partial Echo | No | No |
| | TE | Shortest (<110ms) | Shortest (<110ms) |
| | Flip Angle | 90° | 90° |
| | TR | 10,000ms | 10,000ms |
| | Halfscan factor | ≥0.62 | ≥0.62 |
| | Water-Fat shift (in phase dir) | Minimum (~11xAcqVoxel size) | Minimum (~24xAcqVoxel size) |
| Fat suppression | No | No | |
| Diffusion Mode | DWI | DWI | |
| Direction | “M,P,S” (i.e. non-Overplus) | “M,P,S” (i.e. non-Overplus) | |
| b-values (user-defined) | 0, 500, 900, 2000 | 0, 500, 900, 2000 | |
| Average high b-values | No | No | |
| PNS Mode | High | High | |
| Gradient Mode | Maximum | Maximum | |
| NSA (averages) | 1 | 1 | |

| | | |
|-----------------------------|----------------------------------------------------|----------------------------------------------------|
| Images | M (magnitude) | M (magnitude) |
| Preparation phases | Full for 1 st scan; Auto for scan 2,3,4 | Full for 1 st scan; Auto for scan 2,3,4 |
| EPI 2D Phase Correction | No | No |
| Save Raw Data | No | No |
| Geometry Correction | Default | Default |
| EPI Factor | 67 | 67 |
| Bandwidth in Freq-direction | 1534 Hz | 1414 Hz |
| Scan Duration | ~2min/scan; 4scans for ~8min total | ~2min/scan; 4scans for ~8min total |

968

| Acquisition Device | Settings Compatible with Conformance | | |
|--------------------|-----------------------------------------|----------------------|----------------------|
| Siemens | <i>Submitted by: Siemens Healthcare</i> | | |
| | Model / Version | Magnetom Aera / VD13 | Magnetom Skyra/ VD13 |
| | Field Strength | 1.5T | 3T |
| | Receiver Coil | <u>HE1-4</u> | <u>HE1-4</u> |
| | Slice Orientation | Transaxial | Transaxial |
| | FOV read and phase | 220mm | 220mm |
| | Base resolution | 130 | 130 |
| | Phase resolution | 100% | 100% |
| | Recon Voxel Size | 0.8x0.8x4mm | 0.8x0.8x4mm |
| | PAT Mode | GRAPPA, PE factor=2 | GRAPPA, PE factor=2 |
| | Phase enc Direction | A >> P | A >> P |
| | Ref lines PE | 40 | 40 |
| | Reference scan mode | Separate | Separate |
| | Qty Slices | 25 | 25 |
| | Phase oversampling | 0% | 0% |
| | Slice Thickness | 4mm | 4mm |
| | Distance Factor | 25% | 25% |
| | Shim mode | Standard | Standard |
| | Mode | 2D | 2D |
| | Multi-slice mode | Interleaved | Interleaved |
| | EPI factor | 130 | 130 |
| | Free Echo Spacing | Off | Off |
| | Echo spacing | 0.77ms | 0.94ms |
| | TE | 98ms | 104ms |
| | TR | 10,000ms | 10,000ms |
| | Fat suppression | No | No |
| | Diffusion Mode | Orthogonal | Orthogonal |
| | Diff. weightings | 4 | 4 |
| | b-value 1,2,3,4 | 0, 500, 900, 2000 | 0, 500, 900, 2000 |
| | Diff. weighted images | On | On |
| | Trace weighted images | On | On |
| | Gradient Mode | Fast | Fast |
| | Averages | 1 | 1 |
| Averaging mode | Long term | Long term | |
| Concatenations | 1 | 1 | |

| | | |
|-------------------|--------------------------------------|--------------------------------------|
| MTC | Off | Off |
| Magn. preparation | None | None |
| Filter | DistortionCorr(2D); PrescanNormalize | DistortionCorr(2D); PrescanNormalize |
| Reconstruction | Magnitude | Magnitude |
| Bandwidth | 1538 Hz/Px | 1424 Hz/Px |
| RF pulse type | Normal | Normal |
| Scan Duration | ~2min/scan; 4scans for ~8min total | ~2min/scan; 4scans for ~8min total |

969

| Acquisition Device | Settings Compatible with Conformance | | |
|------------------------|--------------------------------------------------------------------------------|------------------------------------|---------------------------|
| General Electric | <i>Submitted by: Memorial Sloan Kettering Cancer Center; and GE Healthcare</i> | | |
| | Model / Version | Optima MR 450 / DV23.1 | Discovery MR 750 / DV23.1 |
| | Field Strength | 1.5T | 3T |
| | Receiver Coil | <u>8HRBrain</u> | <u>8HRBrain</u> |
| | Slice Orientation | Transaxial | Transaxial |
| | FOV | 22cm | 22cm |
| | Phase FOV | 100% | 100% |
| | Acquisition matrix | 128x128 | 128x128 |
| | Acq voxel size | 1.72x1.72x4mm | 1.72x1.72x4mm |
| | Recon voxel size | 0.98x0.98x4mm | 0.98x0.98x4mm |
| | ASSET Acceleration, Phase | 2 | 2 |
| | Freq enc Direction | R/L | R/L |
| | Qty Slices | 25 | 25 |
| | Slice Thickness | 4mm | 4mm |
| | Slice spacing | 1mm | 1mm |
| | Shim | Auto | Auto |
| | Imaging Options | 2D, spin-echo, EPI, DIFF | 2D, spin-echo, EPI, DIFF |
| | Num Shots | 1 | 1 |
| | Dual Spin Echo | No | No |
| | TE | Min Full (~123ms) | Min Full (~104ms) |
| | TR | 10,000ms | 10,000ms |
| | Fat suppression | No | No |
| | Diffusion Direction | ALL | ALL |
| | b-value | 0, 500, 900, 2000 | 0, 500, 900, 2000 |
| | Phase Correct | On | On |
| | dB/dt control mode | 1 st | 1 st |
| | NEX | 1 | 1 |
| Bandwidth | Default (250kHz) | Default (250kHz) | |
| 3D Geometry correction | No | No | |
| Scan Duration | ~2min/scan; 4scans for ~8min total | ~2min/scan; 4scans for ~8min total | |

970

971 **Appendix E: Technical Assessment Procedures**

972 Procedures below are for basic assessment of MRI equipment in conformance to the quantitative DWI
 973 Profile. Conformance limits for performance metrics are suggested to ensure that technical
 974 measurement errors related to the MRI system do not unduly contribute to measurement variance.

975 E.1. ASSESSMENT PROCEDURE: ADC QUALITIES AT/NEAR ISOCENTER

976 This activity describes criteria that are necessary for an MRI system to meet the quantitative DWI Profile
977 Claims.

978 *E.1.1 Discussion*

979 To assess an MRI system for ADC measurement bias and precision, a phantom containing media having
980 known diffusion properties is required. Water maintained at 0°C is widely used as a known standard with
981 diffusion coefficient = 1.10×10^{-3} mm²/s, and is the basis for ice water-based DWI phantoms [68-70]. This
982 assessment procedure requires the assessor have access to an ice water DWI phantom, such as the QIBA
983 DWI phantom [111] or alternative that contains a measurement sample of water (≥ 30 mL volume) located
984 at isocenter surrounded by an ice water bath [68-70]. The assessor must allow sufficient time for the
985 sample to achieve thermal equilibrium (≥ 1 hour) and the phantom must contain an adequate volume of
986 ice to surround the measurement sample over the entire MRI exam period. Details for preparation and
987 use of the QIBA DWI phantom are available in the QIBA DWI wiki. This assessment procedure requires
988 the assessor follow the core DWI scan parameters defined in Appendix D, Table 2, which involves
989 acquisition of diffusion weighted images of the phantom at nominal b -values = 0, 500, 900, 2000 s/mm².

990 Typically, MRI systems exhibit best performance at or near isocenter where ADC bias reflects overall
991 calibration of gradient amplitude and DWI sequence timing. For this procedure, proximity to isocenter is
992 to be determined by location of the center of an ROI used to assess ADC. Spatial coordinates of the ROI-
993 center are often available using the scanner's electronic caliper read-out of ROI-center coordinates in the
994 patient-based frame of reference defined by assessor's "Patient Landmark" location. Note, the patient-
995 based frame and magnet-based frame (true isocenter) may not be synonymous, and displacement
996 between the two may vary from scan series to scan series. To maintain minimal offset between patient-
997 based and magnet-based frames, the assessor shall define the "Patient Landmark" on the center of the
998 phantom then keep the prescription of slices used for quantitative assessment centered on
999 Superior/Inferior=0 mm (for cylindrical bore magnets). For this procedure, an ROI having center
1000 coordinates $[RL, AP, SI]$ is "at isocenter" when $\sqrt{RL^2 + AP^2 + SI^2} \leq 4$ cm, and the maximum diameter
1001 of the ROI ≤ 2 cm. A minimum ROI diameter of ~ 1 cm will provide sufficient number of pixels (>80) for
1002 adequate sampling of phantom ADC heterogeneity for reliable estimate of within ROI statistics (standard
1003 deviation and mean). For uniform analysis, "QibaPhanR1.4" software provided through the QIDW can be
1004 used to generate the relevant ADC ROI assessment metrics (bias, precision, repeatability and SNR) for
1005 QIBA DWI phantom, as described below.

1006 The QIBA DWI phantom, and other water-based phantoms are isotropic so measured diffusion coefficient
1007 should be independent of applied diffusion gradient direction. Throughout this profile and assessment
1008 procedure, "DWI" will refer to the composite of three orthogonal DWIs as the trace DWI.

1009 Two or more diffusion weightings are required to calculate ADC, and full ADC maps are generated on a
1010 pixel-by-pixel basis (though low SNR may bias these pixel-by-pixel ADC maps) using the mono-exponential
1011 model:

$$1012 \quad ADC_{bmin,b} = \frac{1}{(b-bmin)} \ln \left[\frac{S_{bmin}}{S_b} \right], \quad \text{EQ(1)}$$

1013 where S represents the diffusion weighted image intensity and subscripts refer to b -value. For this
1014 assessment procedure, if only two b -values are used, they must include the nominal minimum b -value in
1015 the calculation, typically $b=0$. If all b -values are used in the ADC calculation, a mono-exponential signal
1016 decay versus b -value model fit (e.g., least-squares) must be used. To achieve adequate diffusion contrast

1017 for ADC estimation via EQ(1), $(b - b_{min})$ shall be ≥ 400 s/mm².

1018 The estimate of MRI system ADC bias in measurement of 0°C water ($DC_{true} = 1.1 \times 10^{-3}$ mm²/s [68]) at
1019 isocenter shall be calculated as:

1020
$$ADC \text{ bias estimate} = \mu - DC_{true}; \text{ or } \%bias = \frac{100\%(\mu - DC_{true})}{DC_{true}}, \quad EQ(2)$$

1021 where μ is the ROI mean of the ADC map at isocenter and the ROI contains 80-150 pixels. Assuming the
1022 pixel values follow a normal distribution, the 95% confidence interval (CI) for this bias estimate is,

1023
$$ADC \text{ bias estimate} \pm 1.96 \frac{\sigma}{\sqrt{N}}, \quad EQ(3)$$

1024 where σ is the standard deviation of ADC pixel values in the ROI containing N pixels.

1025 The standard deviation of ADC pixel values within an isocenter ROI is one indicator of random
1026 measurement error (precision) in ADC maps expressed as a percentage relative to the ROI mean (%CV) as:

1027
$$ADC \text{ error estimate} = 100\% \cdot \frac{\sigma}{\mu} \quad EQ(4)$$

1028 Similar to ADC bias estimate, this procedure typically uses an ROI of ~ 1 cm² (>80 pixels) on a water sample
1029 at 0 °C (e.g. center tube of QIBA DWI phantom) at isocenter, and follow the QIBA DWI phantom scan
1030 protocol to estimate ADC error.

1031 The established QIBA DWI phantom scan protocol is to acquire four DWI scans (each ~ 2 minutes) in
1032 immediate succession holding acquisition conditions constant. This procedure serves multiple aims: (1)
1033 inspect for monotonic trend in ADC vs time suggesting the phantom was not at thermal equilibrium; (2)
1034 inspect for artifact or drift suggesting system instability; (3) allow for estimation of voxel signal-to-noise
1035 ratio (SNR); and (4) provide an estimate of short-term (intra-exam) repeatability [68, 70]. Repeated
1036 scanning of the phantom over multiple days/weeks/months more closely resembles serial scanning of
1037 patients in longitudinal studies. Regardless of interval over which repeated measurements are performed,
1038 assuming normally distributed measures, the Repeatability Coefficient (RC) and “within-subject”
1039 Coefficient of Variation as a percentage (wCV) are calculated as [30, 35, 36]:

1040
$$RC = 2.77 \cdot \sigma_w; \quad wCV = 100\% \frac{\sigma_w}{\mu}, \quad EQ(5)$$

1041 where σ_w^2 is the within-subject (phantom) parameter variance and μ is the parameter mean. The average
1042 of repeated ROI means at isocenter and square root of variance of these means may be used in EQ(5) to
1043 estimate RC and wCV as a metric of system technical performance. Please note, phantom-based RC and
1044 wCV derived here are under relatively ideal conditions and should not be taken as representative of
1045 repeatability achieved in human DWI/ADC studies that involve more sources of variability.

1046 *E.1.2 Specification*

1047

| Parameter | Actor | Requirement |
|----------------------------|-------|--------------------------------------------------------------------------------------------------------------|
| ADC bias at/near isocenter | | $ ADC \text{ bias} \leq 0.04 \times 10^{-3} \text{ mm}^2/\text{s}$, or $\leq 3.6\%$ per instructions above |
| ADC error at/near | | ADC random error $\leq 2\%$ per instructions above |

| | | |
|----------------------------------------------------------------------------|-----------------------------------------------------|------------------------------------------------------------------------------------------------|
| isocenter | Acquisition Device / Physicist / Scientist | |
| Short-term (intra-exam) ADC repeatability at/near isocenter | | $RC \leq 1.5 \times 10^{-5} \text{ mm}^2/\text{s}$ and $wCV \leq 0.5\%$ per instructions above |
| Long-term (multi-day) ADC repeatability at/near isocenter | | $RC \leq 6.5 \times 10^{-5} \text{ mm}^2/\text{s}$ and $wCV \leq 2.2\%$ per instructions above |

1048

1049 E.2. ASSESSMENT PROCEDURE: DWI SIGNAL TO NOISE

1050 This activity describes criteria that are necessary for an MRI system to meet the Profile Claim. This
 1051 procedure can be used by a vendor or an imaging site to estimate relative signal-to-noise ratio (SNR) of an
 1052 MRI system in the context of DWI and parametric ADC maps (both for phantom and subjects).

1053 *E.2.1 Discussion*

1054 Signal-to-noise ratio of any MR image is heavily dependent on acquisition conditions so while SNR is
 1055 informative of system performance, its assessment by the suggested procedure is not an absolute system
 1056 performance metric. Determination of SNR by this procedure serves two aims: (1) provide a relative
 1057 system performance metric; and (2) confirm SNR was adequate to measure ADC bias without incremental
 1058 bias due to low SNR.

1059 This procedure is used to assess SNR at the acquisition voxel level. Common filtering, interpolation and
 1060 reconstruction algorithms lead to correlated noise in neighboring DWI pixels. Therefore, the described
 1061 procedure relies on analysis that yields a noise estimate averaged over an ROI to mitigate effect of
 1062 correlated noise.

1063 Signal estimated as the mean pixel intensity value over an ROI is straightforward; however, DWI noise
 1064 estimation is more difficult. Using standard deviation of pixel values in signal-free background (i.e. air) as
 1065 noise estimate is unreliable due to commonly-used parallel imaging reconstruction, coil-sensitivity
 1066 equalization routines and Rician bias of “magnitude” signals [92-94, 112]. Instead for this procedure,
 1067 noise will be estimated by the temporal change in pixel values measured over multiple scans. The QIBA
 1068 DWI phantom scan protocol requires four scans repeated in immediate succession holding all acquisition
 1069 conditions constant. Images containing the measurement ROI over these four dynamics shall be visually
 1070 inspected for conspicuous (multi-pixel) spatial shift, distortion, or artifact in any of the dynamics.
 1071 Assuming none, random noise is considered to be the main contributor to scan-to-scan differences. To
 1072 assess noise by this procedure, software (similar to “QibaPhanR1.4”) must be available to combine
 1073 dynamic images and calculate the temporal standard deviation of each pixel (i.e. over the “n” dynamic
 1074 scans). An image comprised of the temporal standard deviation of pixel values shall be referred to as the
 1075 “temporal noise image”. An image comprised of the temporal mean of pixel values shall be referred to as
 1076 the “signal image”. Note, an image comprised of the pixel-by-pixel division of the signal image by the
 1077 temporal noise image is referred to as the “signal-to-fluctuation-noise-ratio image” [113], but this should
 1078 not be used to estimate SNR. Instead, the calculation estimates noise as spatial mean within an ROI of

1079 temporal noise image and corresponding signal as a spatial ROI mean of the temporal average signal image
 1080 [112]:

1081
$$SNR_{nDyn} = \frac{\text{Spatial mean pixel value on Signal Image}}{\text{Spatial mean pixel value on Temporal Noise Image}} \quad \text{EQ(6)}$$

1082 The 95% confidence interval for this SNR estimate is $\pm 1.96 \frac{\sigma_{SNR}}{\sqrt{N}}$,

1083 where $\sigma_{SNR} = SNR_{nDyn} \sqrt{sCV^2 + nCV^2}$ is the “error propagation” estimate of standard deviation of SNR
 1084 pixel values in an ROI containing N pixels with spatial coefficients of variance, sCV and nCV , for the
 1085 temporal average signal image and temporal standard-deviation noise image, respectively.

1086 An alternative procedure to estimate SNR from an even quantity of dynamic scans is to first sum all odd-
 1087 numbered dynamics called “sumODD image” and sum all even-numbered dynamics called “sumEVEN
 1088 image”, then create their difference called “DIFF image” = sumODD – sumEVEN. Using these, an estimate
 1089 of SNR within an ROI from n -dynamic scans acquired in immediate succession holding conditions fixed
 1090 shall be calculated as [113]:

1091
$$altSNR_{nDyn} = \sqrt{n} \frac{\text{Spatial mean pixel value on Signal Image}}{\text{Spatial standard deviation pixel value on DIFF Image}} \quad \text{EQ(7)}$$

1092 EQ(7) shall be used when only two dynamic scans ($n=2$) are available.

1093 For conditions defined in this assessment procedure (i.e. 4 dynamics and 80-100 pixel ROIs) equation EQ(6)
 1094 tends to overestimate SNR slightly although has tighter confidence interval relative to equation EQ(7).
 1095 The choice of which equation to use may depend on capabilities of the analysis software. SNR analysis via
 1096 equations EQ(6) and/or EQ(7) may be performed on source DWI images, as well as on derived ADC maps.

1097 In situations where two or more dynamic series are not available, the “noise” level may be crudely
 1098 estimated (i.e. still subject to Rician bias and background regularization) by the standard deviation in
 1099 signal-free background or by the standard deviation within the ROI defined on uniform signal-producing
 1100 area. Prior to defining the background ROI, the assessor must inspect the images with a tight
 1101 window/level and strive to select a background region that contains uniform random noise while avoiding
 1102 signal gradients, structured noise (e.g. ghosts) or severely modulated zones (often masked to “zero”).
 1103 While considered unreliable for reasons stated above, the equation to estimate SNR of an ROI in signal-
 1104 producing region relative to background region is:

1105
$$SNR_{vs\ bkgnd} = \frac{\text{Spatial mean pixel value on Signal Image}}{\text{Spatial standard deviation pixel value in background ROI}} \quad \text{EQ(8)}$$

1106 Since performed on magnitude images, this procedure under-estimates noise thus over-estimates SNR.
 1107 This Rician bias may be predicted using DWI DRO and could be appropriately factored into further analysis
 1108 of ADC statistics [92, 93, 112].

1109 At a minimum, the assessment procedure outlined in EQ(6) and EQ(7) shall be performed on the $b=0$
 1110 diffusion weighted image. Low SNR conditions can introduce bias in ADC measurement (see Figure E.1).
 1111 To be conformant with this profile and avoid introduction of bias due to low SNR conditions, an MRI
 1112 system shall have $SNR \geq 50 \pm 5$ for the $b=0$ image in an ROI of 1 cm diameter (80-100 pixels). This SNR will
 1113 allow measurement of mono-exponential diffusion media having diffusion coefficients $\leq 1.1 \times 10^{-3} \text{ mm}^2/\text{s}$
 1114 (e.g. water at 0 °C) using b -values $\leq 2000 \text{ s}/\text{mm}^2$ and avoid incremental bias due to noise. SNR limits for
 1115 different ADC and b -value ranges relevant for clinical trials can be assessed using DWI DRO provided
 1116 through QIDW (Figure E.1).

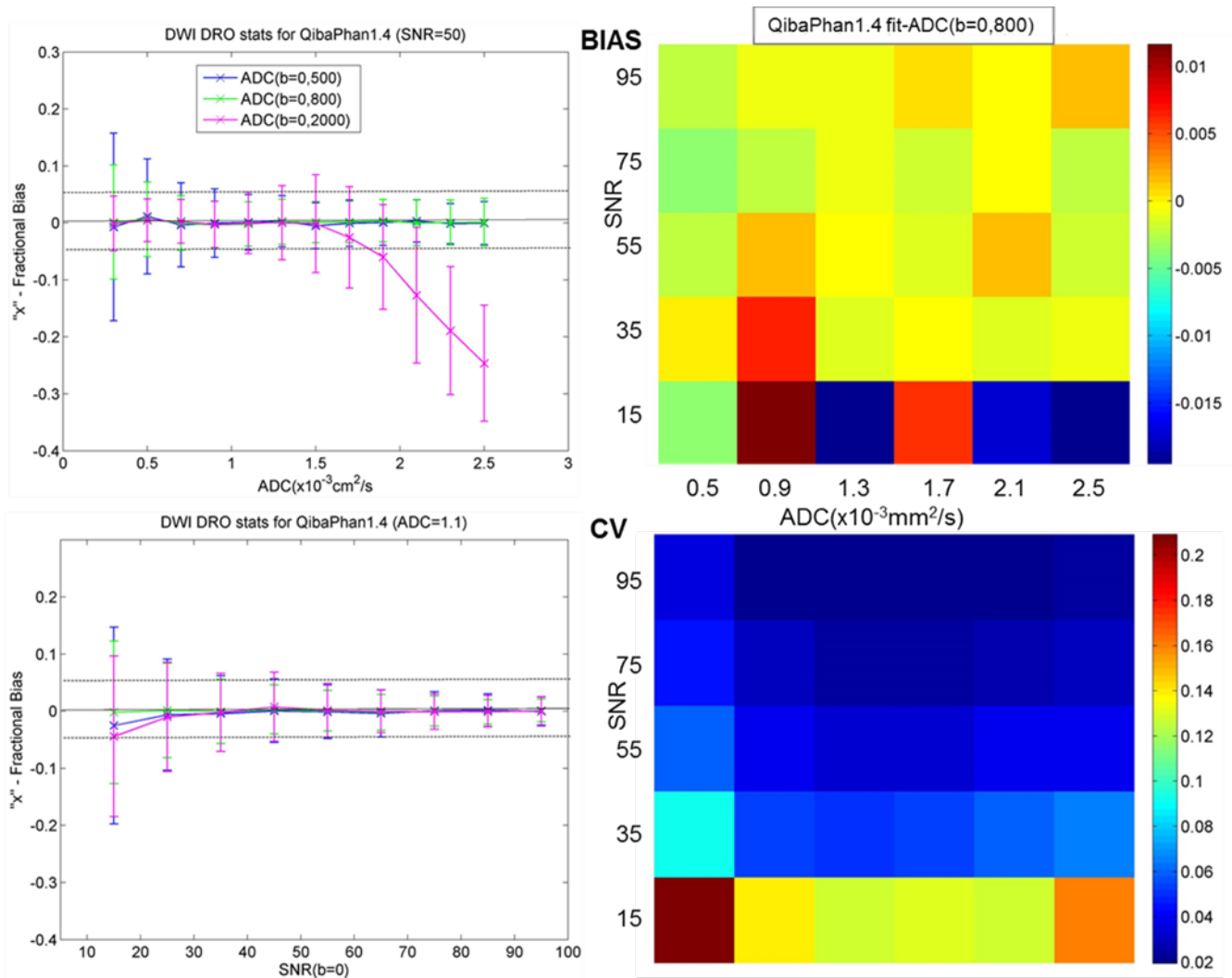


Figure E.1: Examples of fractional-bias and CV metrics for DWI-DRO ADC maps generated using QibaPhan1.4 SW. Left panes show fractional ADC bias and SD (error-bars) as a function of true (i.e., DRO input) ADC (top: at SNR=50) and SNR (bottom: at ADC=1.1 $\times 10^{-3} \text{mm}^2/\text{s}$) for three b-values (color-coded in legend). The dotted horizontal lines mark $\pm 5\%$ deviation to guide optimal DWI parameter ranges for ADC, SNR, b-value. Mean bias appears to be dependent on ADC and b-value and independent of SNR, while bias SD closely follows CV-trend and mostly SNR-dependent. Right panes show the SNR/ADC maps for mean bias and CV metrics at b-value=800 (typical of liver DWI protocol), indicating that the fit-ADC bias error (mean +/- SD) falls within +/-5% for SNR>50 in liver ADC range (0.7-1.7) $\times 10^{-3} \text{mm}^2/\text{s}$.

1117

1118 *E.2.2 Specification*

1119

| Parameter | Actor | Requirement |
|-------------|------------------------------------------------|---------------------------------------------------|
| DWI b=0 SNR | Acquisition Device / Image Analyst / Scientist | SNR (b=0) $\geq 50 \pm 5$ per instructions above. |

1120

1121

1122 E.3. ASSESSMENT PROCEDURE: ADC *b*-VALUE DEPENDENCE

1123 This activity describes criteria that are necessary for an MRI system to meet the Profile Claims. This
 1124 procedure can be used to document artefactual *b*-value dependence in ADC measurements.
 1125

1126 *E.3.1 Discussion*

1127
 1128 The QIBA DWI phantom and other ice water phantoms *should* exhibit mono-exponential signal decay with
 1129 increasing *b*-value. Any apparent change in measured ADC with choice of *b*-value suggests one or
 1130 combination of the following: (1) output gradient amplitude is not linear with input demand; (2)
 1131 background gradients that have substantial but variable contribution to the actual *b*-value; (3) spurious
 1132 signal in *b*≈0 DWI that is eliminated at moderately low *b*-values (e.g. *b*≥50 s/mm²); and (4) inadequate SNR
 1133 at high *b*-values. To assess whether an MRI system exhibits artefactual *b*-value dependence in ADC
 1134 measurement, the assessor shall compare ADC values measured at isocenter on an ice water phantom as
 1135 a function of *b*-value pairs described in equation 1. The lowest *b*-value (typically *b*_{min} = 0) must be included
 1136 in each *b*-value pair. The assessor shall calculate *b*-value dependence as:

$$ADC \text{ bvalue dependence} = 100\% \left\| \left\| \frac{(ADC_{b_{min},b_2} - ADC_{b_{min},b_1})}{ADC_{b_{min},b_1}} \right\| \right\|, \quad EQ(9)$$

1138 where *b*₂ ≠ *b*₁. Note, adequate diffusion contrast is required for ADC estimation via EQ(1), therefore both
 1139 (*b*₁ - *b*_{min}) and (*b*₂ - *b*_{min}) shall be ≥ 400 s/mm².
 1140

1141 *E.3.2 Specification*

| Parameter | Actor | Requirement |
|--------------------------------|-----------------------------------------------------|------------------------------|
| ADC <i>b</i> -value dependence | Acquisition Device / Physicist / Scientist | < 2% per instructions above. |

1144 E.4. ASSESSMENT PROCEDURE: ADC SPATIAL DEPENDENCE

1145 This activity describes criteria that are necessary for an MRI system to meet the Profile Claim. This
 1146 procedure can be used to document artefactual spatial non-uniformity of ADC measurements.
 1147

1148 *E.4.1 Discussion*

1149
 1150 All ADC calculations described above utilize nominal *b*-values entered by the assessor during DWI
 1151 acquisition and retained in DICOM headers. In turn, *b*-value selection determines amplitude and timing
 1152 of diffusion-encoding gradient pulses within the diffusion sequence. Due to current physical constraints
 1153 of gradient designs, gradient strength is not spatially uniform throughout the imaged volume. The
 1154 greatest contributor to non-uniformity in ADC maps is gradient nonlinearity (GNL), although other sources
 1155 such as uniformity of the main magnetic field can also contribute to spatial ADC bias at off-center locations
 1156 [72-75, 114]. Regardless of source, the maximum level of allowable ADC spatial non-uniformity of an MRI
 1157 system depends on scale of the imaging volume for the specific clinical application. For example, DWI
 1158 studies dedicated to the prostate or brain lesions could benefit from relatively minimal expected GNL
 1159 spatial bias when the imaging prescription requires the lesion be located near superior/inferior = 0mm;

1160 whereas bilateral breast or unilateral off-center liver DWI will likely experience greater GNL bias. For MRI
 1161 system performance assessment, a DWI phantom should be selected that reasonably spans the imaging
 1162 volume of the associated clinical application and that preferably fits in the same application-specific
 1163 receiver coil. By its physical nature (determined by gradient coil design), spatial non-uniformity GNL bias
 1164 is expected to be independent of b -value and ADC range. Thus, assessment of this bias for phantom is a
 1165 reasonable estimate for bias in patient scans in clinical trials. In the context of clinical trial, GNL non-
 1166 uniformity bias is expected to increase both the ROI ADC error (i.e. in ROI mean and ADC histogram width,
 1167 and increasing wCV), and the variability among systems.

1168 The assessor shall use a DWI phantom having known diffusion coefficient, such as the QIBA DWI phantom
 1169 or other suitable ice water-based phantom, follow established phantom preparation instructions, and
 1170 acquire DWI using a protocol matched to the associated application. Using EQ(2), ADC bias shall be
 1171 assessed in multiple ROIs of at least 80 pixels each that reasonably sample spatial offset(s) from magnet
 1172 isocenter anticipated for the specific clinical application. Maximum allowed bias for a system compliant
 1173 to this profile will increase with maximum allowed offset from isocenter. For MRI systems conformant to
 1174 this profile, maximum allowed bias for select spatial offsets are illustrated in specifications below.

1175 *E.4.2 Specification*

1176

| Parameter | Actor | Requirement |
|----------------------------------------------------------------------------|-----------------------------------------------|-------------|
| Maximum bias with offset from isocenter: within 4 cm in any direction | Acquisition Device / Physicist / Scientist | < 4% |
| Right or Left < 10 cm with A/P and S/I <4 cm | | < 10% |
| Anterior or Posterior < 10 cm with R/L and S/I <4 cm | | < 10% |
| Superior or Inferior < 5 cm with R/L and A/P <4 cm | | < 10% |

1177

1178 Note that with other performance assessment metrics conformant to the Profile, the listed acceptable
 1179 ranges for ADC non-uniformity bias could be the major source of the technical measurement error (both
 1180 for wCV and mean ADC bias) limiting ADC confidence intervals.

1181